Modified BART for Learning Heterogeneous Effects in Regression Discontinuity Designs

Rafael Alcantara [*] Meijia Wang [†] P. Richard Hahn [†] Hedibert Lopes [*]

July 2, 2024

Abstract

This paper introduces BART-RDD, a sum-of-trees regression model built around a novel regression tree prior, which incorporates the special covariate structure of regression discontinuity designs. Specifically, the tree splitting process is constrained to ensure overlap within a narrow band surrounding the running variable cutoff value, where the treatment effect is identified. It is shown that unmodified BART-based models estimate RDD treatment effects poorly, while our modified model accurately recovers treatment effects at the cutoff. Specifically, BART-RDD is perhaps the first RDD method that effectively learns conditional average treatment effects. The new method is investigated in thorough simulation studies as well as an empirical application looking at the effect of academic probation on student performance in subsequent terms data (Lindo et al., 2010).

Keywords: Bayesian causal forest, tree ensembles, regression discontinuity design

[*] Insper

[†] Arizona State University

1 Introduction

In an RDD, deterministic treatment assignment implies that conditional confoundedness is trivially satisfied, given the running variable. However, controlling for the running variable introduces a complete lack of overlap. Thus, identification of treatment effects from RDDs relies on assumptions that permit coping with this lack of overlap. First, individuals are unable to manipulate their realization of the forcing variable. For example, if the forcing variable is a test score and students can take the test only once, then students who score slightly above or below the cutoff are likely very similar except for their position relative to the cutoff. On the other hand, if students could retake the test arbitrarily often, then a student who scored above the cutoff on their first try and a student who did so only on their tenth try are most likely not similar, but both would be eligible for treatment. Second, the conditional expectation of the response variable, given the forcing variable, must be smooth at the cutoff point. Without this assumption, it would not possible to disambiguate between a treatment effect and non-causal aspect of the data-generating process (Lee and Lemieux, 2010; Imbens and Lemieux, 2008).

This paper investigates the use of Bayesian additive regression tree models (Chipman et al., 2010; Hahn et al., 2020) for the purpose of fitting RDD data with additional covariates for estimating conditional average treatments effects (CATE) at the cutoff. Broadly, our work expands on both frequentist and Bayesian methods for performing RDD analyses that incorporate covariates in addition to the running variable. Relative to earlier works, the method proposed here accommodates a richer set of data generating processes and admits more convenient sensitivity analysis and methods for visualizing heterogeneity. Most importantly, our estimator is one of the few RDD estimators which allow for exploring heterogeneity in a data-driven manner, instead of relying on separate ATE estimation for predetermined subgroups.

1.1 Previous work

The inclusion of covariates in RDD models has been studied by Calonico et al. (2019), who extend the local linear regression to include covariates linearly and discuss the implications of this in terms of bias and variance, and Frölich and Huber (2019) who propose a nonparametric kernel regression method which increases precision and may reduce bias and restore identification in data with discontinuities in the covariate set at the threshold, provided that all relevant discontinuous covariates are included. Additionally, Arai et al. (2021) and Kreiss and Rothe (2023) study RDD regressions with high-dimensional covariate sets. The latter two essentially consist of a pre-selection step where one fits a variable selection model (typically a Lasso) to either the full sample or a subsample closer to the cutoff and then fits the local polynomial estimator of Calonico et al. (2019) to the reduced feature set. These methods inherit the local polynomial's linearity assumption which can lead to high variance estimators in the presence of strong heterogeneity if the running variable and other features interact in more complex ways. The estimator proposed by Frölich and Huber (2019) is more flexible in that regard because it allows for feature-specific kernels, extending the traditional local RDD regression. However, this can render the method computationally infeasible as the dimension of the feature set increases.

The previous works discuss inclusion of covariates from a perspective of obtaining precision gains and barely discuss effect moderation. Regarding effect heterogeneity, Frandsen et al. (2012) and Shen and Zhang (2016) discuss it from the perspective of distributional effects, while Cattaneo et al. (2016) and Bertanha (2020) discuss heterogeneity arising from settings with multiple cutoffs. These works do not focus specifically on heterogeneity in the form of moderation by additional variables. Becker et al. (2013) extend the traditional local regression to include interaction terms between the running variable and additional features. Hsu and Shen (2019) develop hypothesis tests for detecting effect moderation in the local regression setup by means of comparison between the ATE parameter for the whole sample and pre-specified subgroups of interest. These methods still depend on reasonable previous knowledge about potential sources of heterogeneity.

Prominent examples of Bayesian estimators for RDDs, include Chib et al. (2023), who estimate the response curves with global splines where observations are weighted by their distance to the cutoff; Karabatsos and Walker (2015), who propose approximating the conditional expectations by an infinite mixture of normals; and Branson et al. (2019), who propose a Gaussian process prior for the expectations, in which observations are also weighted by their distance to the cutoff. All of these methods consist of global approximations of the outcome curves, while in some cases emphasizing units near the cutoff to obtain better predictions in that region. As will be discussed later, our method can be seen as an intermediate approach between such global approximations and the local linear regression ubiquitous in the frequentist literature, since we use the entire data to estimate the outcomes but take advantage of the local nature of BART for estimation near the cutoff.

Reguly (2021) proposes what is perhaps the closest in spirit to our method. The author proposes a modification to the basic Classification and Regression Tree (CART) algorithm in which the tree is split using all features available except for the running variable. Then, within each leaf the algorithm performs a separate regression for treated and untreated units, and the leaf-specific ATE parameter is obtained as the difference between the intercepts of the two regressions. The model can be seen as a non-linear polynomial regression where the parameters depend on the covariates via the CART fit. This approach presents two important differences compared to ours. First, it is a single tree method, whereas we propose a forest model. Second, the flexibility of the tree is only used for the additional covariates, but the leaf regressions are still polynomials of the running variable. These features mean that, although more flexible than global regressions, the method should still suffer in situations where the response surface is smoother on the covariates or where the way the running variable interacts with the others is more complex than a polynomial model could accurately capture. Still, this is, to the best of our knowledge, the only RDD estimator beside our own which does not require pre-specification of subgroups for CATE analysis.

2 Background

This paper brings together ideas from many different areas, each with their own terminology and notation. In this section we review the basics of regression discontinuity designs, BART, and Bayesian causal forests.

2.1 Regression Discontinuity Designs

Following Imbens and Lemieux (2008), we frame the RD setting in a potential outcomes model, which can be briefly described as follows. Let Z denote a binary treatment variable and Y_i^z denote the potential outcome of unit i under treatment state $Z_i = z$. The treatment effect for unit i is defined as:

$$\tau_i \coloneqq Y_i^1 - Y_i^0. \tag{1}$$

Let X denote the running variable and W denote a set of additional covariates. Commonly, interest lies on the average and conditional average treatment effect (ATE/CATE):

$$\begin{aligned} \mathbb{E}[\tau_i] &= \mathbb{E}[Y_i^1 - Y_i^0] \\ \mathbb{E}[\tau_i \mid X, W] &= \mathbb{E}[Y_i^1 - Y_i^0 \mid X, W]. \end{aligned} \tag{2}$$

These quantities are of course unobservable since each unit is only observed at a single given treatment state. However, under the following assumptions we can link τ to the observed outcome and covariates (Y, Z, X, W).

Assumption 2.1 (SUTVA) *This assumption has two components: consistency and no-interference, which are represented, respectively, as:*

$$\begin{aligned} &Y = Y^0 + Z(Y^1 - Y^0) \\ &Y_i^1, Y_i^0 \perp\!\!\!\perp Z_j, \end{aligned} \tag{3}$$

for all $i, j \in \{1, \ldots, n\}$, where $i \neq j$.

Assumption 2.2 (Mean conditional unconfoundedness) *Y^1, Y^0 are mean independent of Z conditional on X, W:*

$$\begin{aligned} \mathbb{E}[Y^1 \mid Z, X, W] &= E[Y^1 \mid X, W] \\ \mathbb{E}[Y^0 \mid Z, X, W] &= E[Y^0 \mid X, W]. \end{aligned} \tag{4}$$

Assumption 2.3 (Conditional overlap) *Both treatment states have a positive probability conditional on X, W:*

$$0 < P(Z = z \mid X, W) < 1. \tag{5}$$

Consistency means perfect compliance, so the observed outcome for an individual that is assigned to treatment is actually his potential outcome under treatment. If there is non-compliance, the outcome observed for an individual under some treatment assignment could actually be his potential outcome under the contrary treatment assignment if he is not a complier. The no-interference condition means that an individual's outcome is only affected by their own treatment status, so there are no spillovers of effects between individuals.

Under these assumptions, we obtain:

$$\mathbb{E}[Y^1 - Y^0 \mid X, W] = \mathbb{E}[Y \mid Z = 1, X, W] - \mathbb{E}[Y \mid Z = 0, X, W]. \tag{6}$$

The distinctive feature of the RDD is that Z is a deterministic function of X:

$$Z_i = \begin{cases} 0, & \text{if} \quad X_i \quad < c \\ 1, & \text{if} \quad X_i \quad \geq c \end{cases}$$

for a known cutoff value c[1].

The deterministic assignment mechanism implies that controlling for X is sufficient to ensure unconfoundedness. However, this control induces a complete lack of overlap. Therefore, treatment effect estimation in the RDD requires additional assumptions to circumvent this issue. In order to discuss these assumptions, we write the expectation of Y given (X, W, Z) as:

$$\begin{aligned} \mathbb{E}[Y \mid X, W, Z] &= \mu(X, W) + \tau(X, W)Z \\ \mu(X, W) &= \mathbb{E}[Y \mid X, W, Z = 0] \\ \tau(X, W) &= \mathbb{E}[Y \mid X, W, Z = 1] - \mathbb{E}[Y \mid X, W, Z = 0]. \end{aligned} \tag{7}$$

Under unconfoundedness, $\tau(X, W)$ identifies the CATE function. However, because of the lack of overlap, one never observes $\mu(X, W)$ and $\tau(X, W)$ simultaneously in any region of the support of (X, W), so that inference about $\tau(X, W)$ is infeasible without further assumptions. We now discuss the kinds of assumptions necessary to obtain identification in the RDD and the type of estimands that can be identified.

For some $\epsilon > 0$, let $x_\varepsilon^- = \{x \in (c - \epsilon, c)\}$, $x_\varepsilon^+ = \{x \in [c, c + \epsilon)\}$, and $x_\epsilon = x_\epsilon^- \cup x_\epsilon^+$. Suppose that, for $X \in x_\epsilon$, the treatment effect function is independent from the treatment variable conditional on X. Then:

$$\begin{aligned} &\mathbb{E}[\mathbb{E}[Y \mid X, W, Z = 1] \mid X, X \in x_\epsilon] - \mathbb{E}[\mathbb{E}[Y \mid X, W, Z = 0] \mid X, X \in x_\epsilon] \\ =&\mathbb{E}[\tau(X, W) \mid X, X \in x_\epsilon^+] + (\mathbb{E}[\mu(X, W) \mid X, X \in x_\epsilon^+] - \mathbb{E}[\mu(X, W) \mid X, X \in x_\epsilon^-]). \end{aligned} \tag{8}$$

Suppose that:

$$\begin{aligned} \mathbb{E}[\mu(X, W) \mid X, X \in x_\epsilon^+] = \mathbb{E}[\mu(X, W) \mid X, X \in x_\epsilon^-] = \mathbb{E}[\mu(X, W) \mid X, X \in x_\epsilon] \\ \mathbb{E}[\tau(X, W) \mid X, X \in x_\epsilon^+] = \mathbb{E}[\tau(X, W) \mid X, X \in x_\epsilon^-] = \mathbb{E}[\tau(X, W) \mid X, X \in x_\epsilon]. \end{aligned} \tag{9}$$

Then, the ATE[2] is identified inside this region:

$$\begin{aligned} &\mathbb{E}[\mathbb{E}[Y \mid X, W, Z = 1] \mid X, X \in x_\epsilon] - \mathbb{E}[\mathbb{E}[Y \mid X, W, Z = 0] \mid X, X \in x_\epsilon] \\ =&\mathbb{E}[\tau(X, W) \mid X, X \in x_\epsilon]. \end{aligned} \tag{10}$$

This is the basis of the continuity-based identification approach introduced by Hahn et al. (2001).

[1] Our focus lies on the so-called “sharp” RDD, in which case there is perfect compliance — as opposed to the “fuzzy” RDD, in which case compliance is imperfect — so the perfect compliance assumption is implicit throughout the text.

[2] As is commonly done in the RDD literature, we refer to the CATE conditional only on X as the ATE and use CATE only when conditioning on W as well

Under that setting, if these conditions can be assumed to hold at least as $\epsilon \to 0$ — *i.e.* if the expectation of the μ and τ functions are continuous at $X = c$ — the ATE at this point is identified as $\mathbb{E}[\tau(X = c, W)]$.

If interest lies in identification of the CATE in some region of the feature set $W = w$, we need similar assumptions about the expectations conditional on W. Suppose that, for all $x_- \in x_\epsilon^-$ and $x_+ \in x_\epsilon^+$:

$$\begin{aligned} \mu(X = x_-, W = w) &= \mu(X = x_+, W = w) \\ \tau(X = x_-, W = w) &= \tau(X = x_+, W = w). \end{aligned} \tag{11}$$

Then, the CATE at $W = w$ is identified in the region x_ϵ by $\tau(X, W = w)$. As before, if these equalities hold as $\epsilon \to 0$, *i.e.* if μ and τ are continuous at $X = c$, the CATE for $W = w$ is identified at that point. Because we propose an estimator for the CATE, (11) is assumed to hold for the remainder of the text. However, it is worth emphasizing that only (9) is required for identification of the ATE, so that, even if $\tau(X, W)$ does not identify any CATE, estimates of this function can still be used to produce ATE estimates if the relevant assumptions hold.

Note that the above assumptions are necessary for identification and not estimation. In particular, it is important to emphasize that $\tau(X = c, W)$ is never observed, only $\mu(X = c, W) + \tau(X = c, W)Z$ and estimation of the CATE (or ATE) relies necessarily on extrapolation of the two conditional expectations at the cutoff. In section 3, we discuss why off-the-shelf BART implementations tend to perform poorly in that task and how we modify the BART prior to improve extrapolation accuracy.

2.2 Bayesian Additive Regression Trees

The Bayesian Additive Regression Trees model (Chipman et al., 2010), or BART, represents an unknown mean function as a sum of regression trees, where each regression tree is assumed to be drawn from the tree prior described in Chipman et al. (1998). Letting $f(x) = \mathbb{E}(Y \mid X = x)$ denote a smooth function of a covariate vector X, the BART model is traditionally written

$$\begin{aligned} Y_i &= f(x_i) + \varepsilon_i, \\ &= \sum_{j=1}^{k} g_j(x_i; T_j, \mathbf{m}_j) + \varepsilon_i, \end{aligned} \tag{12}$$

where $\varepsilon_i \sim \mathrm{N}(0, \sigma^2)$ is a normally distributed additive error term. Here, each $g_j(x; T_j, \mathbf{m}_j)$ denotes a piecewise function of x defined by a set of splitting rules T_j that partitions the domain of x into disjoint regions, and a vector, $\mathbf{m}_j$, which records the values $g(\cdot)$ takes on each of those regions. Therefore, the parameters of a standard BART regression model are $(T_1, \mathbf{m}_1), \dots, (T_k, \mathbf{m}_k)$ and σ. Chipman et al. (2010) consider priors such that: the tree components $(T_j, \mathbf{m}_j)$ are independent of each other and of σ^2, and the terminal node parameters $\mu_{k1}, \dots, \mu_{kb}$ of a given tree k are independent of each other. Furthermore, Chipman et al. (2010) consider the same priors for all trees and leaf node parameters. The model thus consists of the specification of three priors: $p(T)$, $p(\sigma^2)$ and $p(\mathbf{m}|T)$.

The tree prior, $p(T)$, is defined by three components. First, the probability that a node d will split is determined by

$$\frac{\alpha}{(1+d)^{\beta}}, \quad \alpha \in (0,1), \beta \in [0,\infty). \tag{13}$$

That is, the deeper the node (higher d), the higher the chance that it is a terminal node. This is essentially a regularization component of the tree prior to avoid overfitting.

The other components of the tree prior are the probability that a given variable will be chosen for the splitting rule at node d, and the probability that a given observed value of the chosen variable will be used for the splitting rule. The splitting variable is chosen uniformly among the set of covariates and then the splitting value is chosen uniformly among the discrete set of observed values of that covariate.

For further details and justication concerning BART prior specification, see Chipman et al. (2010).

2.3 Bayesian Causal Forest

There are two common strategies for estimating heterogeneous treatment effects. One is to simply focus on estimating the response surface including a treatment indicator as an additional covariate, while the other consists of fitting two different models for treatment and control groups. Recently, these approaches have been dubbed “S-learners” and “T-learners” respectively, where S means “single” and T means “two” (Künzel et al., 2019). In the context of applying BART for causal inference, Hill (2011) follows the first approach, under the assumption of no unobserved confounding, which implies that treatment effect estimation reduces to response surface estimation. For the second approach, one could simply fit two different BART models for treated and control units.

As described in Hahn et al. (2020), neither of these approaches is ideal in common causal inference settings. The two-model T-learner approach has the problem that regularization of the treatment effect is necessarily weaker than regularization of each individual model, which is the opposite of what you would expect in many contexts, where treatment effects are expected to be modest. The single-model approach of Hill (2011) addresses this to some extent, but at the expense of transparency: the implied degree of regularization depends sensitively on the joint distribution of the control variables and the treatment variable. Accordingly, Hahn et al. (2020) proposed the Bayesian Causal Forest (BCF) model, which fits two BART models simultaneously to a reparametrized response function:

$$\begin{aligned} &Y_i = \mu(X_i, \mathrm{w}_i) + \tau(X_i, \mathrm{w}_i) b_{z_i} + \varepsilon_i, \quad \varepsilon_i \sim N(0, \sigma^2), \\ &b_0 \sim \mathrm{N}(0, 1/2), \quad b_1 \sim \mathrm{N}(0, 1/2). \end{aligned} \tag{14}$$

where $\mu(\cdot)$ is referred to as a prognostic function and $\tau(\cdot)$ a treatment effect function[3]. The model parametrized in this way can be seen as a linear regression with a covariate-dependent slope and intercept (Hahn et al., 2020).

Note that b_0 and b_1 are parameters that can be estimated; practically this is desirable because it avoids giving the treated potential outcome higher prior predictive variance[4]. Under this parameter-

[3] This terminology is motivated by the case where $b_0 = 0$ and $b_1 = 1$, in which case $\mu(x) = \mathbb{E}(Y^0 \mid X = x)$ and $\tau(x) = \mathbb{E}(Y^1 \mid X = x) - \mathbb{E}(Y^0 \mid X = x)$.

[4] Treatment coding can imply non-equivalent priors for the treatment effects. For example, $Z \in (0,1)$ implies the expected potential outcomes for the treated group depend on the treatment effect function, while the expected potential outcomes for the control group do not, which is not reasonable if we have a comparison between two levels of treatment

ization the treatment effect can be expressed as:

$$\mathbb{E}(Y^1 \mid X = x) - \mathbb{E}(Y^0 \mid X = x) = (b_1 - b_0)\tau(x). \tag{15}$$

2.4 The XBCF model

To sample from the posterior distributions of trees, Chipman et al. (2010) propose a backfitting MCMC algorithm that explores the tree space by proposing at each iteration a grow or prune step, producing highly correlated tree samples. This can make convergence of the algorithm slow and may not scale well to large datasets. And, as BCF depends on BART priors, it will also be affected by these problems.

As a more efficient alternative, He and Hahn (2023) propose the accelerated Bayesian additive regression trees (XBART) algorithm for BART-like models. XBART grows new trees recursively, but stochastically, at each step while using a similar set of cutpoints and splitting criteria as BART, which allows for much faster exploration of the posterior space. Krantsevich et al. (2023) extends the XBART algorithm to the BCF model, with their accelerated Bayesian causal forest (XBCF) algorithm, an XBCF algorithm. The XBCF algorithm uses a slightly modified BCF model, allowing the error variance to differ by treatment status:

$$\begin{aligned} Y_i &= a\mu(x_i) + b_{z_i}\tilde{\tau}(x_i) + \epsilon_i, \quad \epsilon_i \sim N(0, \sigma^2_{z_i}) \\ a &\sim \mathrm{N}(0,1), \quad b_0, b_1 \sim \mathrm{N}(0, 1/2), \end{aligned} \tag{16}$$

where $\mu(x)$ and $\tilde{\tau}(x)$ are two XBART forests and $\tau = (b_1 - b_0)\tilde{\tau}$.

The BART-RDD method described below is a modified XBCF algorithm, specialized in critical ways to the RDD setting. The key innovation from He and Hahn (2023) is the so-called "Grow-From-Root" stochastic tree-fitting algorithm, reproduced in algorithm 1 in a summary form. It will be discussed later how this algorithm is particularly well-suited to the RDD context.

3 Bayesian Regression Trees for Regression Discontinuity Designs

Just as BCF was developed to address shortcomings of off-the-shelf BART implementations for treatment effect estimation assuming conditional unconfoundedness, here we propose to modify the BCF model to cope with challenges that are unique to regression discontinuity designs. First, note that a BART-based T-learner will not work well because it is not a continuous model and therefore the limit-based identification arguments don't apply. A BART-based S-learner similarly fails because it contains the T-learner as a submodel (if the first split is on Z); more generally, a split at $X = c$ and a split on Z are indistinguishable, meaning that treatment effect estimation is going to be sensitively affected by the priors over cutpoints in hard-to-understand ways.

To overcome these limitations we introduce novel splitting constraints. At a high level, the strategy is to ensure that the data used to make predictions at $X = c$ warrant a causal interpretation. In terms of the model, this means that $\mu(x = c, w)$ and $\tau(x = c, w)$ must be composed of trees where

instead of treatment *vs.* no treatment. See Hahn et al. (2020) for a more thorough discussion on how treatment effect priors are dependent on treatment encoding.

Algorithm 1: GrowFromRoot

```
   Output: Modifies T by adding nodes and sampling associated leaf parameters $\mu$.
1  if the stopping conditions are met then
2      Go to step 13, update leaf parameter $\mu_{node}$;
3  end
4  $s^{\emptyset} \leftarrow s(y, \mathbf{X}, \mathbf{\Psi}, \mathcal{C}, \text{all})$;
5  for $c_{jk} \in \mathcal{C}$ do
6      $s_{jk}^{(1)} \leftarrow s(y, \mathbf{X}, \mathbf{\Psi}, \mathcal{C}, j, k, \text{left})$;
7      $s_{jk}^{(2)} \leftarrow s(y, \mathbf{X}, \mathbf{\Psi}, \mathcal{C}, j, k, \text{right})$;
8      Calculate $L(c_{jk}) = m\left(s_{jk}^{(1)}; \mathbf{\Phi}, \mathbf{\Psi}\right) \times m\left(s_{jk}^{(2)}; \mathbf{\Phi}, \mathbf{\Psi}\right)$;
9  end
10 Calculate $L(\emptyset) = |\mathcal{C}| \left(\frac{(1+d)^{\beta}}{\alpha} - 1\right) m\left(s^{\emptyset}; \mathbf{\Phi}, \mathbf{\Psi}\right)$;
11 Sample a cutpoint $c_{jk}$ proportional to integrated likelihoods
       $$P(c_{jk}) = \frac{L(c_{jk})}{\sum_{c_{jk} \in \mathcal{C}} L(c_{jk}) + L(\emptyset)},$$
   or
       $$P(\emptyset) = \frac{L(\emptyset)}{\sum_{c_{jk} \in \mathcal{C}} L(c_{jk}) + L(\emptyset)}$$
   for the null cutpoint;
12 if the null cutpoint is selected then
13     $\mu_{node} \leftarrow SampleParameters(\emptyset)$;
14     return
15 else
16     Create two new nodes, left_node and right_node, and grow $T$ by designating them as
         the current node's (node) children;
17     Partition the data $(y, \mathbf{X})$ into left $(y_{left}, \mathbf{X}_{left})$ and right $(y_{right}, \mathbf{X}_{right})$ parts, according
         to the selected cutpoint $x_{ij'} \leq x_{jk}^{*}$ and $x_{ij'} > x_{jk}^{*}$, respectively, where $x_{jk}^{*}$ is the value
         corresponding to the sampled cutpoint $c_{jk}$;
18     GrowFromRoot($y_{\text{left}}, \mathbf{X}_{\text{left}}, \mathbf{\Phi}, \mathbf{\Psi}, d+1, T,$ left_node);
19     GrowFromRoot($y_{\text{right}}, \mathbf{X}_{\text{right}}, \mathbf{\Phi}, \mathbf{\Psi}, d+1, T,$ right_node)
20 end
```

any partition containing the point $(x = c, w)$ has a corresponding function evaluation that has been estimated from causally valid contrasts. Assuming continuous conditional expectations (as is standard in much RDD work), this is possible if the estimation is based on data close enough to the cutoff. The BART-RDD model developed here satisfies this criterion by explicitly imposing it during the tree growing process.

3.1 Splitting Constraints for RDD with Regression Trees

The proposed constraints have two distinct, though related, goals. First, we need the treatment-control contrast – upon which $\tau(x = c, w)$ will be estimated – to be well-defined: for this we require observations from both treatment arms (e.g. overlap). Without imposing this condition it is typical during posterior sampling to encounter leaf nodes that contain no treated (resp. untreated) observations, which in turn yields leaf parameters that are biased for the treatment effect.

Second, because we cannot rely on observations far from the cutoff to estimate the treatment effect, we insist that a partition that includes $x = c$ have a strong majority of its observations within a narrow, user-defined band about the cutoff. This constraint defines a set of suitably *localized* basis functions from which to perform causal inference at the cutoff.

More formally, these constraints can be expressed as follows. For a user-defined bandwidth parameter $h > 0$, we assume that the potential outcome mean function does not vary abruptly inside the interval $[c - h, c + h]$, which we refer to as the "identification strip". Let $B \subset \mathcal{X}$ be a hypercube corresponding to a node in a regression tree and let N_b denote the number of observations falling within B. Further, let n_l denote the number of observations in $B \cap [c - h, c)$ and n_r denote the number of observations in $B \cap [c, c + h]$. For user-specified variables $N_{Omin} \in \mathbb{N}^+$ and $\alpha \in (0, 1)$, the leaf node region B is valid if it satisfies the following condition:

$$\begin{aligned}&\big(\forall w \mid (x = c, w) \notin B\big)\cup \\ &\Big((\exists w \mid (x = c, w) \in B) \cap (\min(n_l, n_r) \geq N_{Omin}) \cap ((n_l + n_r)/N_b \geq \alpha) \Big).\end{aligned} \tag{17}$$

The initial clause says that any node which does not make predictions at the cutoff remains entirely unrestricted; the second clause says that any node that *does* make predictions at $x = c$ has to have both i) a minimum number of observations within the cutoff region on either side of the cutoff, as well as ii) not too many observations, proportionally, outside of the identification strip.

3.2 Stochastic search for valid partitions

For nodes predicting at the cutoff, the two conditions (i and ii) above have qualitatively different ramifications for the stochastic search for valid partitions. In particular, the first condition, if unsatisfied, can never become satisfied by further branching, while the second condition, if unsatisfied, *can* be satisfied by further branching, by trimming away observations outside of the identification strip. This observation motivates us to use XBART/XBCF rather than standard BART MCMC for our model fitting. An unmodified local random walk would violate recurrence because certain valid states can only be reached by passing through invalid states; as a practical matter, reaching valid partitions by a random walk would be highly inefficient. By utilizing the Grow-From-Root algorithm, passing through invalid states to reach favorable valid states is a simple matter of not terminating the growth process at an invalid state. Specifically, never accept a partition that violates condition i, and never stop at a partition that violates condition ii.

In practice, this new stochastic search procedure is implemented by modifying the likelihood calculation in steps 8 and 10 of the GFR algorithm for XBCF as follows. Consider a candidate split with cutpoint c_{jk} which splits the current node into left and right nodes. Let $B_x^{(l)}$ denote the range of x which the left node covers and similarly define $B_x^{(r)}$. Let n_{ll} and n_{lr} denote the number of observations such that $x \in [c-h, c)$ and $x \in [c, c+h]$ in the left node, and n_{rl} and n_{rr} denote the same quantities in the right node, respectively. If,

$$c \in B_x^{(l)} \quad \text{and} \quad \max(n_{ll}, n_{lr}) < N_{Omin} \tag{18}$$

or if

$$c \in B_x^{(r)} \quad \text{and} \quad \max(n_{rl}, n_{rr}) < N_{Omin}, \tag{19}$$

this split violates condition (i). Therefore, we consider this an invalid partition and set $L(c_{jk}) = 0$. If the split does not violate condition (i), we calculate its likelihood as in the GFR algorithm. For condition (ii), we check whether:

$$c \in B_x \quad \text{and} \quad \frac{n_l + n_r}{N_b} < \alpha. \tag{20}$$

If so, we set the likelihood of the no-split option $L(\emptyset) = 0$ unless there are no other valid splits, in which case we set $L(\emptyset) = 1$. In the latter case, we end up with a tree that is still invalid, as it violates condition ii; our implementation monitors for this eventuality and find that it rarely if ever occurs in most data sets.

3.3 Illustration of the constraints and search

The impact of expression (17) on the fitted trees may be visualized by considering a concrete example. Consider a tree fit with only the running variable (X). Figure 1 plots X against some outcome Y for a dataset with 75 observations, presenting different partitions in X. For this example, the cutoff is $c = 0$ – denoted by the dotted line – and the ATE at that point is equal to 0.5. We consider a window of $h = 0.06$, denoted by the dashed lines in the plots. The treated units ($x \geq c$) are denoted by black triangle dots and the control units are denoted by white round dots. Splits in X are denoted by solid lines. For each partition, we represent the inferred potential outcome as a red line for untreated and blue line for treated outcomes. For the partitions that include both types of observations — *i.e.* points from both sides of the cutoff — we represent both potential outcomes.

Panel 1a shows a split which is invalid since it cuts through the identification strip, leading to a node that contains only one point to the right of the cutoff in that region. The ATE at the cutoff for that tree is predicted to be 0.78. Panel 1b presents a split which only violates condition (ii), since it does not cut through the identification strip, but features a node with too many points outside the strip. The ATE at the cutoff for that tree is predicted to be 0.7. This tree can be made valid by 'trimming out' points too far from the cutoff in the right node. Panel 1c presents an additional split that does exactly that. The ATE at the cutoff for that tree is predicted to be 0.67. Finally, panel 1d presents another tree, with a couple of additional splits to the left of the identification strip, and a split to the right that's closer to the strip. Since the new nodes generated do not include the identification strip, they are all potentially valid. The ATE at the cutoff for that tree is predicted to be 0.6.

Analysis of the figures makes clear what types of trees will be accepted under our restrictions. We consider only trees that do not cut through the identification strip, are well populated with points in that region from both sides of the cutoff and are tight around that region. This way, we incorporate the RDD assumption that units sufficiently near the cutoff are similar enough to be compared and use this to create an 'overlap region' around the cutoff. The shape of the trees is also largely dependent on the data structure. If there are many points with $x \approx c$ we can make the identification strip narrower without being too restrictive on the tree growth especially if the points are well dispersed in regards to the other covariates. On the contrary, if most points have x far from the cutoff we might need to define a wider identification strip to reasonably explore the tree space. Finally, it is worth noting that this strategy can be used more generally for any problem where one must fit tree ensembles and enforce smoothness over a specific variable and around a specific point.

This exercise also highlights the problems that unmodified BART models might face in the context of the RDD. Note that all trees above are, at least in principle, valid under the standard BART prior. If the nodes that contain $X = c$ include points close to the cutoff from both sides, but many points far from it, these trees will only lead to reasonable causal contrasts if Y is relatively constant with respect to X. Otherwise, such trees should exhibit strong bias if the prognostic or treatment effect functions have high variance, as is the case in the previous example. In fact, as we move closer towards the kinds of trees that would be accepted by BART-RDD — *i.e.* moving from the first panel to the last — we decrease the bias in the predicted ATE at the cutoff. The important distinction here is that, while all BART-based models could reach reasonable trees, only BART-RDD is guaranteed to do so by rejecting trees that do not behave 'well'. This means the unmodified BART trees might sometimes do well and sometimes not, so these models will produce ensembles which mix over biased and unbiased trees, leading to biased fits.

3.4 Prior specification

The question remains as to how one should set the relevant parameters in order to obtain good predictions. A completely general rule cannot be expected, as the impact each parameter has in the estimation is highly data-dependent. Nonetheless, it is instructive to consider what kinds of restrictions our parameters imply to the tree search process and how they impact prior bias.

First, consider the bandwidth parameter h. On the one hand, h should be set as low as possible for two reasons. First, setting h too high makes it more likely that a given tree would cut through the identification strip. In particular if h is such that the strip covers all the support of X, the algorithm would only accept trees that do not use X for partitions. Given the essential role that X plays in the outcome distribution in an RDD setting, not using it for the tree splits would lead to severely biased trees. Additionally, since the goal is to make inference enforcing smoothness over X at a specific

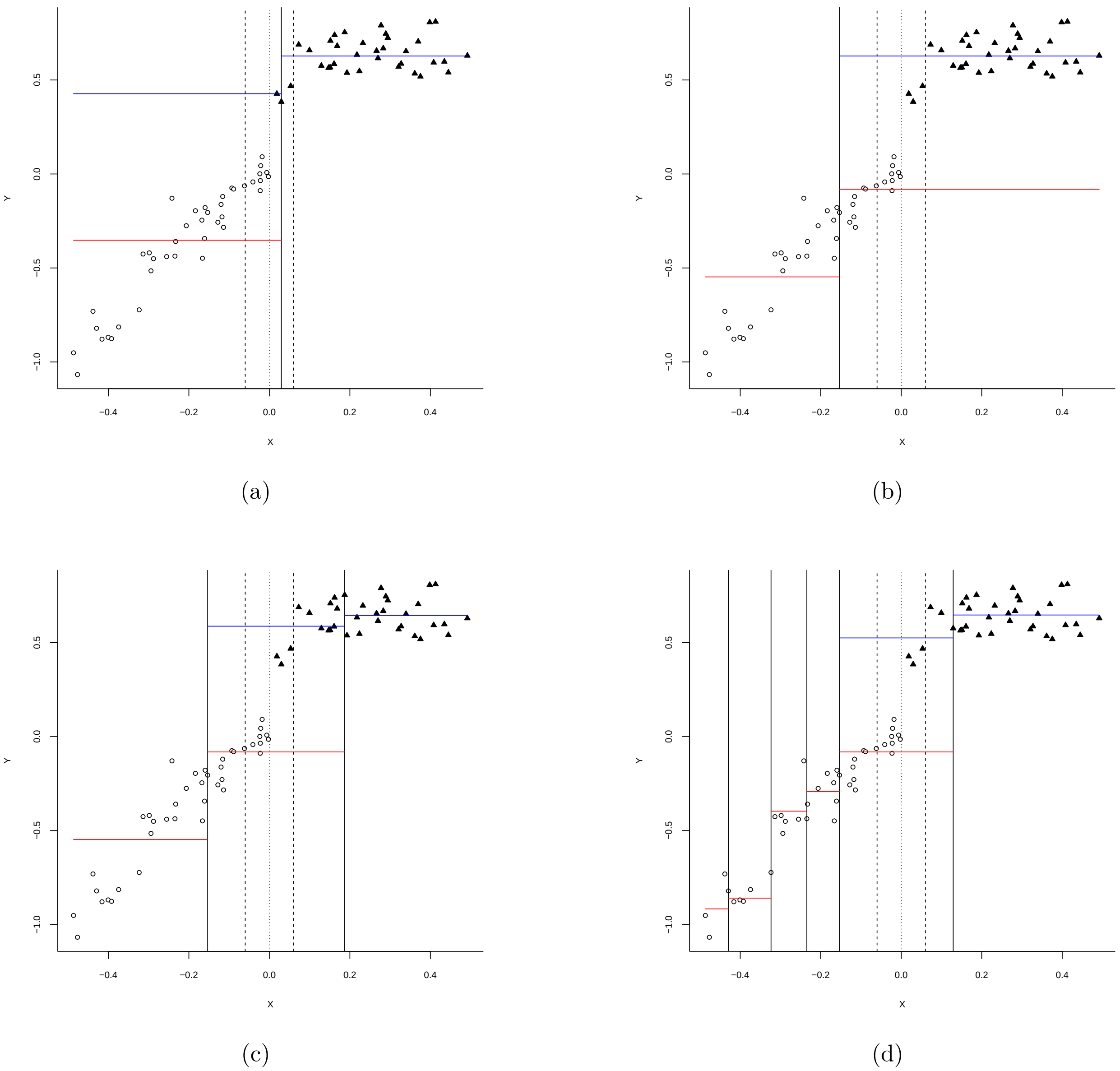

(a)

(b)

(c)

(d)

Figure 1: Tree examples: the first tree shows a split that violates condition i, which cannot be accepted; the second tree presents a split that violates condition ii, which can be accepted because we can make this tree valid by trimming out the region outside the identification strip in the relevant nodes; the third tree is an example of the kind of tree that would be accepted by the algorithm, with tight bounds on the identification region and good representation from both sides of the cutoff; the fourth tree is the same as the third one with some additional splits that do not contain the identification strip, so the tree remains valid

point ($X = c$), one should only use points as close to c as possible to obtain better approximations of the true function around that point.

On the other hand, there is also a limit to how low one can set h for each dataset. In particular, if h is so small that there are no points inside the identification strip, any tree will produce nodes with an empty overlap region and, thus, be invalid. This means that h also interacts with N_{Omin} in that extreme: even if there are points in the identification strip, if there are less than N_{Omin} points, the same phenomenon happens, making all trees invalid.

Next, we turn to N_{Omin}: if it is set to 0, the trees could produce nodes which contain the overlap region but have no points inside it. Thus, predictions near the cutoff could be based only on observations too far from the cutoff, which would undermine the constraint associated with this parameter. Setting N_{Omin} too high could be too restrictive since there would be less valid nodes containing the overlap region, which could bias the individual posterior distributions or at least make it harder to detect heterogeneity in the data, since we could have very short trees.

Finally, we note that if α is set too low, we allow for many points outside the strip to influence the results from nodes that do include the strip. However, setting it high is not necessarily a problem since, as discussed in the previous section, nodes that do not satisfy this criterion can be made to satisfy it by simply 'trimming' the outter region of nodes containing the identification strip. It is important to note, however, that setting α too high could lead to many forced splits in the boundaries of the identification strip, which can lead to an increase in variance if these additional splits are not particularly relevant. Therefore, this parameter should also be chosen carefully.

Clearly, it is nontrivial how these considerations might interact in a given sample. This reflects the immense delicacy of the regression discontinuity design itself, rather than a limitation intrinsic to the BART-RDD proposed; all RDD methods require grappling with how to set tuning parameters. Our proposed approach is via a *prior predictive calibration* procedure. Specifically, we recommend, for a given sample (x, w, y), the following prior ellicitation procedure:

1. Generate s samples of a synthetic data from a known DGP using (x, w)
2. Fit BART-RDD to each sample for different values of the prior parameters
3. Choose the parameter values which lead to lower RMSE values for the ATE in those s synthetic samples.

We find that generating the synthetic data from a simple model with no treatment effect heterogeneity and relatively small ATE leads to finding good values for the prior parameters even when the true data exhibits strong heterogeneity or large effects. This is also a reasonable prior for the treatment effects, unless one has strong reason to believe in a more complex scenario. In the simulation studies to follow, we use this procedure to choose h, N_{Omin} and α. A detailed analysis of this procedure may be found in Appendix A, where we discuss its application in the context of the simulations.

4 Simulation studies

4.1 Setup

In order to investigate the properties of the BART-RDD algorithm, we perform a simulation study comparing its performance to an S-learner BART fit (S-BART), a T-learner BART fit (T-BART), the robust bias-corrected local linear regression (LLR), as implemented by Calonico et al. (2015), and the cubic spline estimator (CGS) of Chib et al. (2023). The goal of this exercise is twofold. First, we want to investigate how BART-RDD compares with off-the-shelf implementations of BART applied to the RDD context. We are able to show that our modification does in fact make the BART prior more suited to this context. Second, we want to compare BART-RDD to estimators that were designed specifically to the RDD context, in particular the local polynomial estimator, by far the most commonly used in the literature, and the cubic splines estimator which is possibly the closest in spirit to that in the Bayesian literature. Besides showing BART-RDD is more suited to the RDD setup than unmodified BART models, we also show that BART-RDD generally performs better and never far worse than the estimators designed specifically for the RDD.

Let X denote the running variable, W an additional set of features, Z the treatment indicator and Y a continuous outcome. We investigate 500 samples of size 1000 of variations of the following DGP:

$$
\begin{array}{lll}
X \sim 2\mathcal{B}(2,4) - 0.75 & Z = \mathbf{1}(X \geq c) & c = 0 \\
W_1 \sim U(-0.1, 0.1) & \mu(X,W) = \dfrac{\mu_0(X,W)}{\sigma(\mu_0(X,W))}\delta_\mu & \bar{\tau} = \{0.2, 0.5\} \\
W_2 \sim \mathcal{N}(0, 0.2) & & \delta_\mu = \{0.5, 1.25\} \\
W_3 \sim \text{Binomial}(1, 0.4) & \tau(X,W) = \bar{\tau} + \dfrac{\tau_0(X,W)}{\sigma(\tau_0(X,W))}\delta_\tau & \delta_\tau = \{0.1, 0.3\} \\
W_4 \sim \text{Binomial}(1, p(x)) & Y = \mu(X,W) + \tau(X,W)Z + \varepsilon & \varepsilon \sim \mathcal{N}(0,1),
\end{array}
$$

where $\mathcal{B}(2,4)$ denotes a Beta distribution with parameters 2 and 4, $p(x)$ denotes the Gaussian probability density of x with mean c and standard deviation 0.5, and:

$$
\begin{aligned}
\mu_0(X,W) &= 3x^5 - 2.5x^4 - 1.5x^3 + 2x^2 + 3x + 2 + \frac{1}{2}\sum_{p=1}^{4}(w_p - E[w_p]) \\
\tau_0(X,W) &= -0.1x + \frac{1}{4}\sum_{p=1}^{4}(w_p - E[w_p])
\end{aligned}
\tag{21}
$$

4.1.1 Rationale

Here we briefly justify the choices made in the simulation design described above. First, although there are other parameters that affect the performance of any estimator, the spread in μ and τ were the only factors that we found to have distinct impacts on different estimators. In other words, the effect of other DGP characteristics in the results were common across estimators in the expected ways[5]. We control these features in the data through the parameters $(\delta_\mu, \delta_\tau)$. The particular choices for these parameters were made in an attempt to replicate realistic behavior in μ and τ. Particularly, we made sure that there are generally no sign changes in the individual treatment effects and that the spread in the prognostic component is larger than the spread in the treatment effects.

In regards to the functional forms chosen, while we did experiment with different functional forms, the results remain the same qualitatively (although sometimes less clear depending on how hard the functions are to estimate). In most methodological RDD studies, the setups considered feature only X as a strong predictor and a very strong signal-to-noise ratio. In that regard, we consider our setup to be more complete in terms of expected characteristics of empirical data[6].

The distribution of X plays an important role in the RDD, as it determines the distribution of treatment. If X is skewed to the left (right) of the cutoff, the sample will have many less (more) treated units, which should make estimation harder. Conversely, if X is nearly symmetric around the cutoff, estimation should be simpler. The distribution described above is relatively standard in the literature, so we chose it for more comparability with previous studies[7]. While we did explore different distributions of X (particularly, centering X further away from the cutoff to either side), these variations did not change the results qualitatively.

4.2 Results

4.2.1 Comparison of ATE Estimates

Although the primary new functionality of BART-RDD is in providing CATE estimates, we begin by examining its performance on the ATE for comparison for other methods and because a good CATE learner should be able to provide ATE estimates as well. Table 1 and figure 2 present the RMSE for the ATE point estimate produced by each estimator[8].

Table 1: RMSE - ATE

$\bar{\tau}$	δ_μ	δ_τ	BART-RDD	S-BART	T-BART	CGS	LLR
0.2	0.5	0.1	0.114	0.214	0.253	0.370	0.233
0.2	0.5	0.3	0.114	0.228	0.264	0.388	0.243
0.2	1.25	0.1	0.226	0.298	0.424	0.411	0.234
0.2	1.25	0.3	0.250	0.321	0.440	0.445	0.255
0.5	0.5	0.1	0.158	0.257	0.249	0.387	0.247
0.5	0.5	0.3	0.147	0.250	0.258	0.372	0.239
0.5	1.25	0.1	0.251	0.397	0.432	0.437	0.251
0.5	1.25	0.3	0.247	0.402	0.429	0.443	0.245

The results indicate that high variation in μ makes estimation harder for all estimators, although

[5] For example, larger sample or effect sizes increased the performance of every estimator in roughly the same manner, meaning these features are not particularly helpful in determining the situations in which the estimators might differ in their performance.

[6] For a summary of the simulation exercises in some of the most relevant methodological RDD papres, see https://github.com/rafaelcalcantara/BART-RDD.

[7] Most papers in fact set $X \sim 2\mathcal{B}(2,4) - 1$. We chose $X \sim 2\mathcal{B}(2,4) - 0.75$ here so that X is centered slightly closer to the cutoff and the proportion of treated and control units in the sample is not so different (we obtain nearly 40% treated units in every sample).

[8] In the case of the Bayesian estimators, we consider the posterior mean as the point estimate.

the difference is not so sizeable for LLR. In that setting, BART-RDD and LLR perform similarly. However, when δ_μ is low, BART-RDD clearly outperforms all estimators. Regarding the other BART-based estimators, S-BART and T-BART perform similarly, but the former is less sensitive to high variability in μ. Overall, CGS is the worst performer in terms of the RMSE.

In order to better understand the behavior of the RMSE, figures 3 and 4 present, respectively, the absolute bias and variance for each estimator, separated by the parameter values of the DGPs. This decomposition highlights some important patterns. First, the consistently low bias of the LLR and CGS estimators is remarkable, which means any variation in their RMSE is coming from the estimator variance. For LLR, this should not come as a surprise given this method's focus on reducing bias, but it is worth noting how effective it is in that regard. On the contrary, BART-RDD presents bias comparable to LLR and CGS when heterogeneity in μ is low, but a much greater bias otherwise. This trend is true for all BART-based models, although, for a given value of δ_μ, BART-RDD almost always presents much lower — and never far worse — bias than the others. Finally, δ_μ is the only factor that significantly affects bias for the BART-based models.

Regarding variance, BART-RDD is always the best performer, with a consistently lower variance than the other estimators. LLR also presents much larger variance than BART-RDD. T-BART presents a slightly larger variance than BART-RDD, whereas S-BART presents larger variance that is very sensitive to δ_μ. Finally, CGS presents the worst variance in all scenarios, which explains this method's poor RMSE performance.

Table 2 presents the coverage rate for each estimator. CGS and LLR present near 95% coverage in all cases, while S-BART presents near 95% coverage in all cases when $\bar{\tau} = 0.2$ and near 90% coverage when $\bar{\tau} = 0.5$. Coverage rates for BART-RDD and T-BART follow a common pattern of decreasing coverage when δ_μ increases. However BART-RDD presents better coverage than T-BART, reaching 95% coverage in one case and never falling below 70% coverage. Meanwhile, T-BART reaches at most 82.8% coverage.

Table 2: Coverage rate for the ATE

$\bar{\tau}$	δ_μ	δ_τ	BART-RDD	S-BART	T-BART	CGS	LLR
0.2	0.5	0.1	0.924	0.954	0.798	0.962	0.940
0.2	0.5	0.3	0.954	0.950	0.724	0.950	0.932
0.2	1.25	0.1	0.782	0.940	0.538	0.970	0.930
0.2	1.25	0.3	0.718	0.950	0.520	0.964	0.938
0.5	0.5	0.1	0.900	0.866	0.828	0.958	0.946
0.5	0.5	0.3	0.920	0.890	0.772	0.962	0.942
0.5	1.25	0.1	0.722	0.870	0.558	0.966	0.918
0.5	1.25	0.3	0.702	0.894	0.572	0.962	0.934

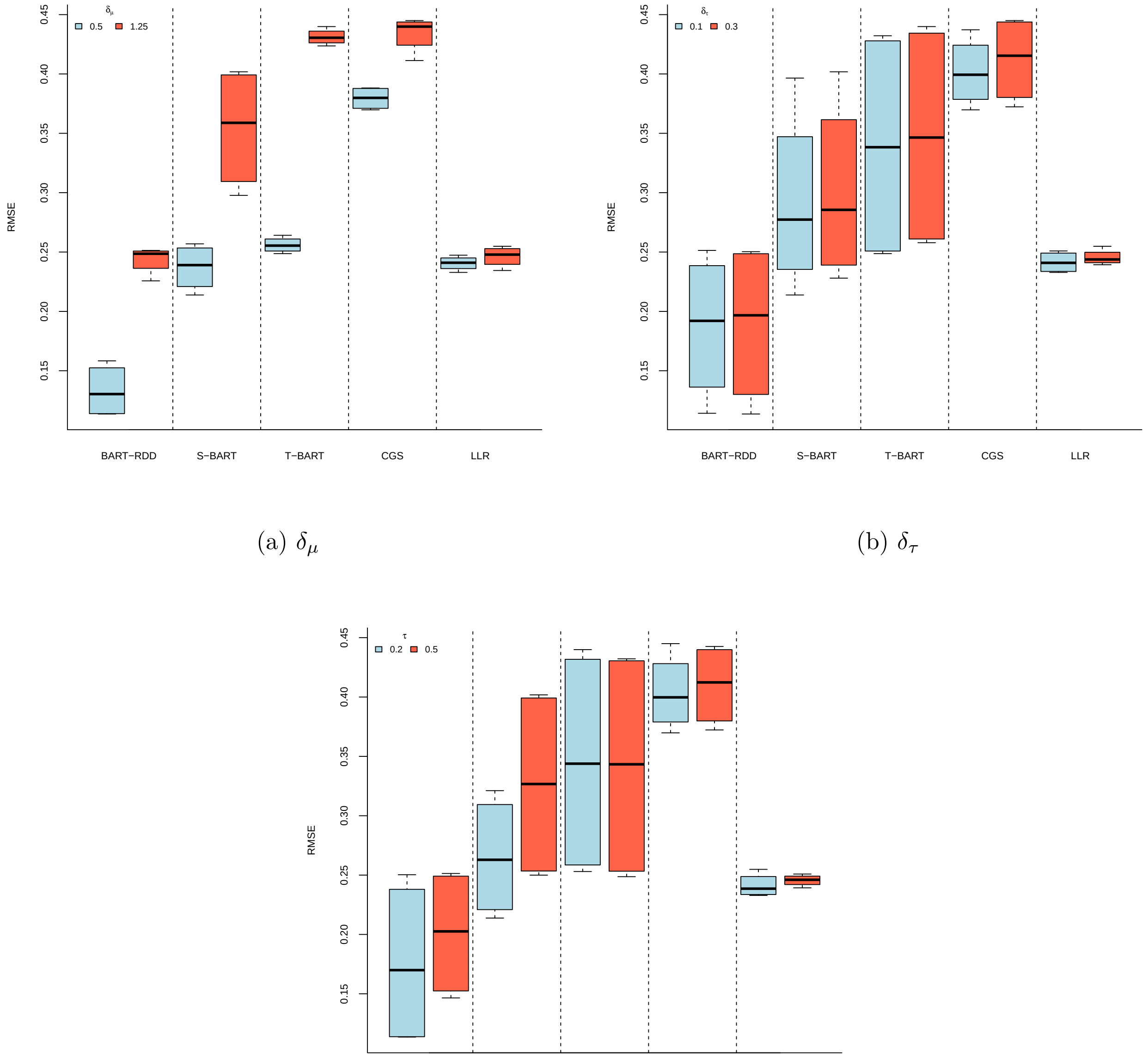

(a) δ_μ

(b) δ_τ

(c) τ

Figure 2: RMSE for the ATE point estimate produced by each estimator, divided by the different DGP parameters

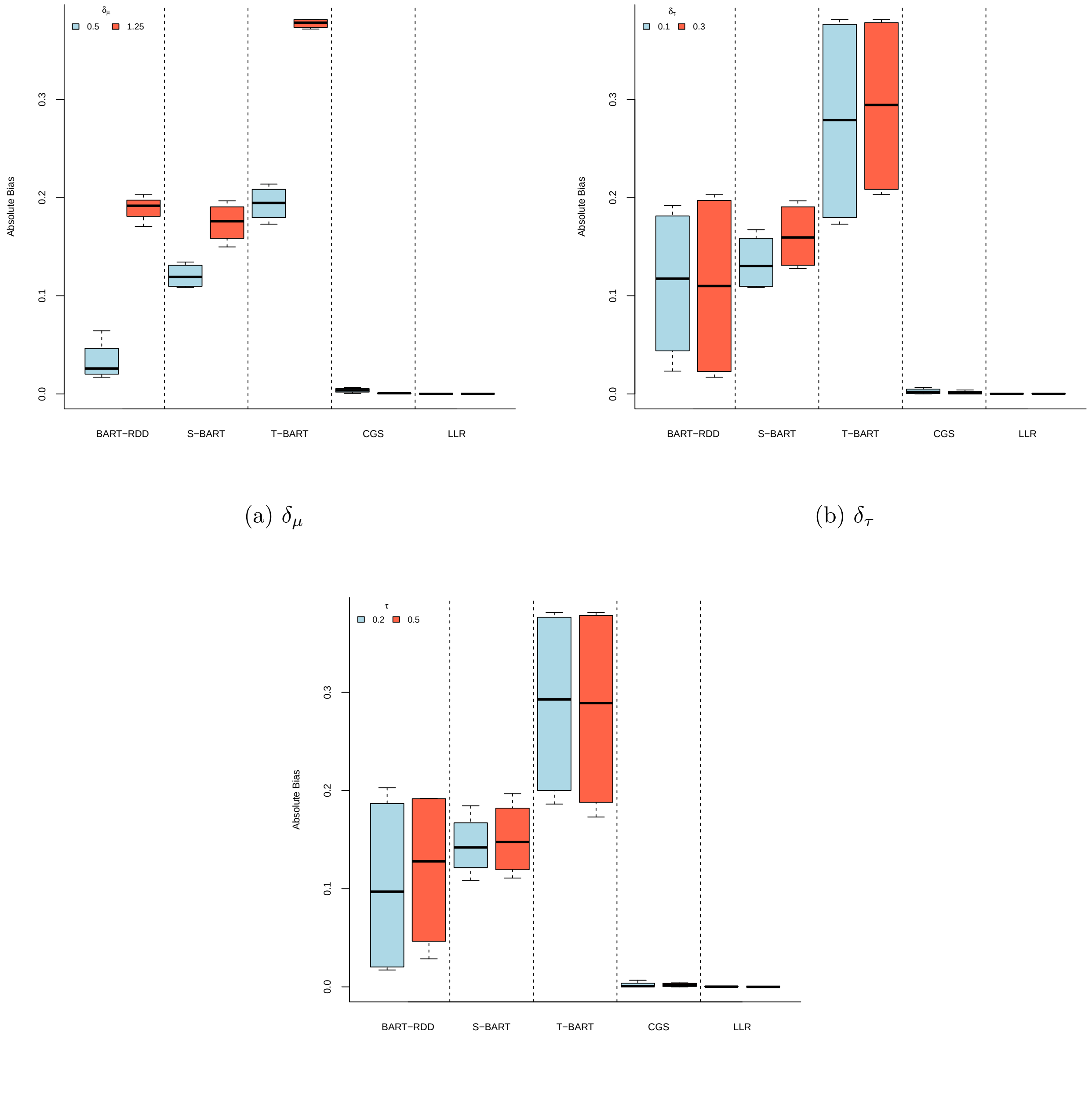

(a) δ_μ

(b) δ_τ

(c) τ

Figure 3: Absolute bias for the ATE point estimate produced by each estimator, divided by the different DGP parameters

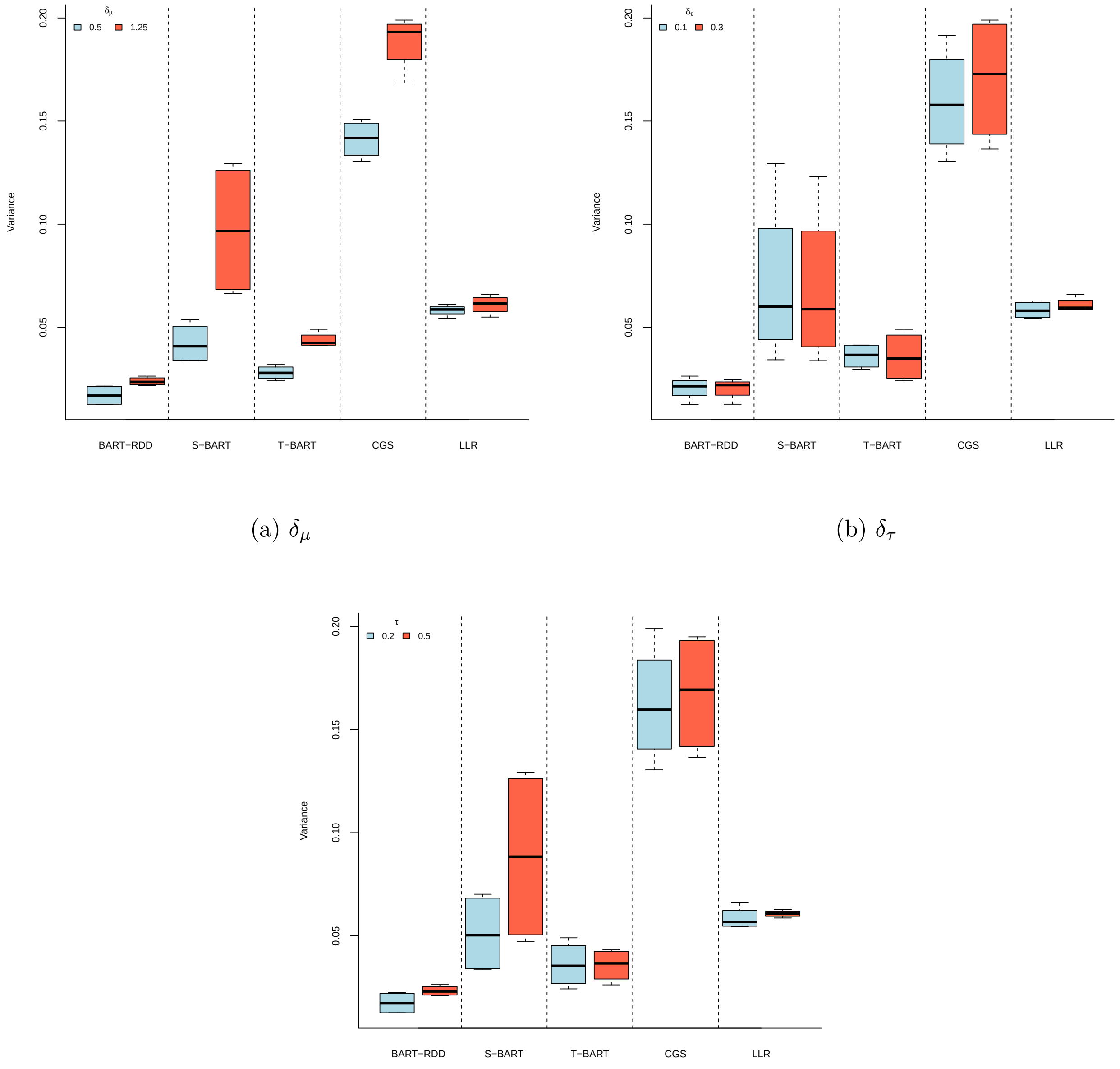

(a) δ_μ

(b) δ_τ

(c) τ

Figure 4: Variance for the ATE point estimate produced by each estimator, divided by the different DGP parameters

Although Bayesian intervals are generally not expected to achieve any particular coverage rate, frequentist coverage is a helpful metric to consider. Table 3 presents a closer look at the intervals produced by each estimator. Comparing the interval sizes provides an explanation of the coverage rate behavior. CGS presents, by far, the largest intervals so it is still able to get good coverage despite being the worst in terms of the RMSE. S-BART produces the second largest intervals on average, which also helps compensate the larger bias in some cases, leading to very good coverage generally. LLR produces the third largest intervals on average, which, combined with the relatively good RMSE performance leads to great coverage. T-BART comes next, and the combination of shorter intervals and bad RMSE performance leads to poor coverage. Finally, BART-RDD produces the shortest intervals. However, because of the really good RMSE performance, it is still able to obtain good coverage in all cases.

Table 3: Interval sizes for the ATE

τ	δ_μ	δ_τ	BART-RDD	S-BART	T-BART	CGS	LLR
0.2	0.5	0.1	0.424	0.713	0.719	1.598	0.855
0.2	0.5	0.3	0.442	0.757	0.677	1.604	0.877
0.2	1.25	0.1	0.546	0.970	0.797	1.792	0.863
0.2	1.25	0.3	0.539	1.068	0.794	1.814	0.880
0.5	0.5	0.1	0.536	0.859	0.743	1.604	0.870
0.5	0.5	0.3	0.519	0.913	0.704	1.607	0.870
0.5	1.25	0.1	0.579	1.239	0.810	1.788	0.870
0.5	1.25	0.3	0.567	1.313	0.818	1.798	0.872

4.2.2 Comparison of CATE estimates

This section compares the various BART-based models in terms of their CATE estimation (the polynomial estimators do not provide CATE estimates). Tables 4 and 5 present the RMSE and coverage for each estimator, respectively. The results for the RMSE are qualitatively the same as before for all estimators. Regarding coverage, BART-RDD is the best model, with S-BART and T-BART performing slightly worse. Overall, these results suggest a similar trend as with the ATE: S-BART and T-BART present similar performance, with the latter being more sensitive to variability in μ. BART-RDD comes out as the best estimator among the BART variants in all scenarios but one.

Table 4: RMSE - CATE

τ	δ_μ	δ_τ	BART-RDD	S-BART	T-BART
0.2	0.5	0.1	0.164	0.204	0.280
0.2	0.5	0.3	0.216	0.287	0.298
0.2	1.25	0.1	0.262	0.255	0.445
0.2	1.25	0.3	0.302	0.345	0.463
0.5	0.5	0.1	0.228	0.247	0.281
0.5	0.5	0.3	0.249	0.297	0.295
0.5	1.25	0.1	0.315	0.363	0.451
0.5	1.25	0.3	0.321	0.411	0.452

Table 5: Coverage - CATE

τ	δ_μ	δ_τ	BART-RDD	S-BART	T-BART
0.2	0.5	0.1	0.993	0.969	0.951
0.2	0.5	0.3	0.986	0.904	0.936
0.2	1.25	0.1	0.985	0.949	0.828
0.2	1.25	0.3	0.974	0.897	0.816
0.5	0.5	0.1	0.986	0.919	0.955
0.5	0.5	0.3	0.985	0.933	0.941
0.5	1.25	0.1	0.980	0.909	0.820
0.5	1.25	0.3	0.982	0.922	0.835

For a more detailed look into the CATE predictions of each model, figures 5 and 6 present the CATE fit for an illustrative sample of the DGP described earlier, with $\delta_\mu = 0.5$ and $\delta_\mu = 1.25$ respectively. We set $\delta_\tau = 0.3$ and $\bar{\tau} = 0.5$ for these examples. The values are presented for units inside the identification strip in ascending order. Two patterns stand out in these comparisons. First, although increasing δ_μ evidently makes it harder to recover τ in general, the results from BART-RDD are a lot less sensitive to these changes. Second, S-BART seems to have a lot more difficulties in picking up variations in W, producing much more constant CATE estimates than the other methods. Overall, the figures suggest that the BART-RDD CATE predictions are less biased and more able to capture heterogeneity than the unmodified BART models.

4.3 Summary of Simulation Results

These simulation results bear out our motivating problem: unmodified BART models have a difficult time coping sensibly with the lack of overlap in RDDs. BART's lack of control over how the leaves containing points near the cutoff are formed can lead to nearly empty nodes in that region. This is especially true if the conditional expectations have a large spread in that region, either because of steepness in X or because of strong heterogeneity in W, as this will probably lead to many splits. These issues arise even more prominently for the T-BART model, since this model only features observations from one side of the cutoff or the other by construction. The BART-RDD model avoids these issues by having direct BART priors for the prognostic and treatment effect components and restricting the growth process of these trees to ensure that nodes containing the cutoff point are well populated by points from both sides of the cutoff.

The effectiveness of BART-RDD in controlling the potential bias of unmodified BART models in the CATE estimation naturally carries over to the ATE estimates. BART-RDD produces ATE estimates that are generally better and never far worse than those produced by the polynomial estimators. Being a Bayesian model for $\mathbb{E}[Y \mid X, W]$, it is expected that BART will control variance at the cost of some bias in the ATE estimation compared to LLR. However, for the reasons discussed above, this bias might be stronger than the variance reduction in the unmodified BART models. BART-RDD, by controlling the extrapolation bias, is able to inherit the good predictive capabilities of BART into this context, leading to competitive ATE estimates, even though the main focus is CATE estimation.

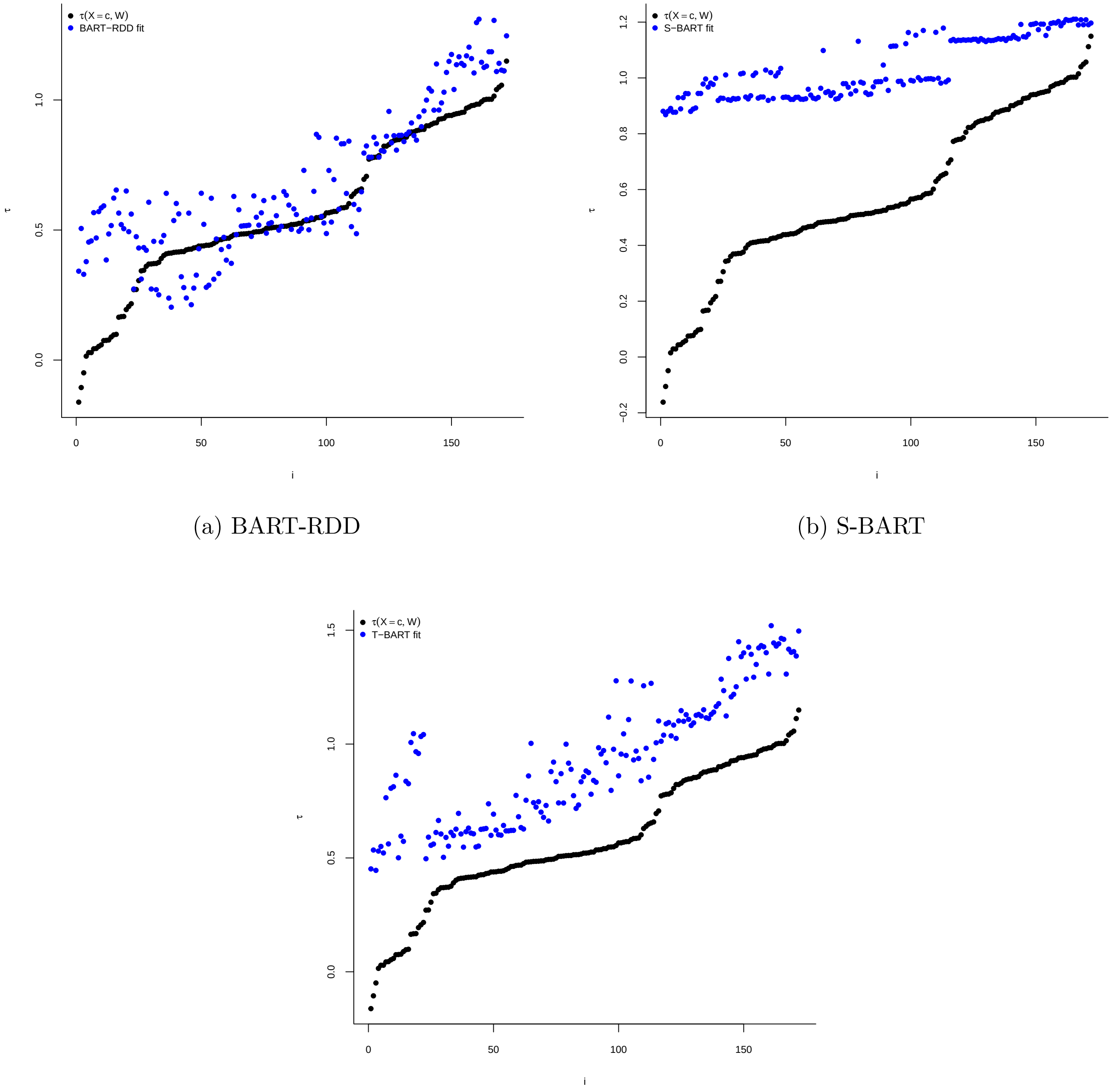

(a) BART-RDD

(b) S-BART

(c) T-BART

Figure 5: Fit for $\tau(X = c, W)$ for each method when $\delta_\mu = 0.5$ versus the true function

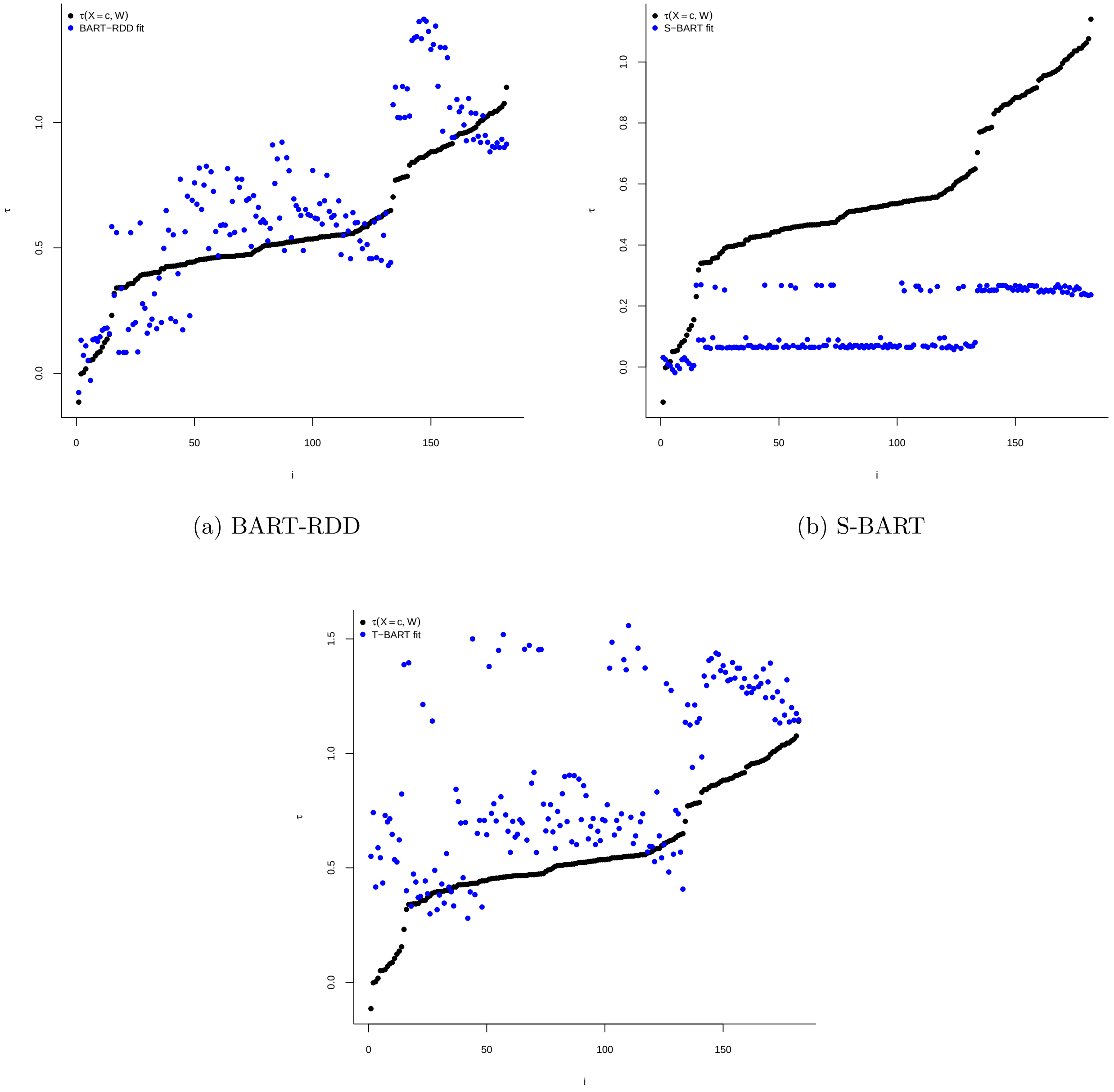

(a) BART-RDD

(b) S-BART

(c) T-BART

Figure 6: Fit for $\tau(X = c, W)$ for each method when $\delta_\mu = 1$ versus the true function

5 The Effect of Academic Probation in Educational Outcomes

We now conclude with a detailed empirical application of BART-RDD to illustrate its usage in a real data setting. The data analyzed in this section comes from Lindo et al. (2010) and consists of information on college students enrolled in a large Canadian university. Students who, by the end of each term, present GPA lower than a certain threshold (which differs between the three university campuses) are placed on academic probation and must improve their GPA in the next term and face threat of punishment if they fail to achieve this goal, which can range from 1-year to permanent suspension from the university.

Among the performance outcomes analyzed by Lindo et al. (2010), we focus on GPA in the term after a student is placed on probation (Y). Following the authors, we define the running variable (X) as the negative distance between a student's first-year GPA and the probation threshold, meaning students below the limit have a positive score and the cutoff is 0. Additional student features in the data include gender ('male'), age when student entered the university ('age_at_entry'), a dummy for being born in North America ('bpl_north_america'), attempted credits in the first year ('totcredits_year1'), dummies for which campus each student belongs to ('loc_campus' 1, 2 and 3), and the student's position in the distribution of high school grades of students entering the university in the same year as a measure of high school performance ('hsgrade_pct').

Figure 7 presents a LOESS fit with a 95% confidence band for the distribution of Y and each covariate conditional on X for $X \in [-0.5, 0.5]$. We see a clear negative relationship between Y and X, meaning students who had a lower GPA in the first year are more likely to have a lower GPA in the second year as well. There is also a clear discontinuity at the probation threshold. Among the covariates, only high-school grades and total credits attempted in the first year have a clear correlation with X, both of them negative. This means that students with low first-year GPA are also more likely to have had bad high-school grades and to have attempted less credits in the first year. The latter feature also presents a discontinuity at the probation threshold, which means it must be included in the estimation to avoid bias.

Table 6 presents the mean, standard deviation, minimum, maximum and correlation with Y for each variable in the full sample and per campus. The running variable, high-school grade percentile and credits attempted seem to be the strongest predictors. In terms of campus composition, the running variable and high-school performance are the only ones with clearly varying distributions across campus. The former feature presents a lower mean for campus 1 compared to the other two, while the latter presents a higher mean for campus 1. This means students in campus 1 generally performed better in high-school and obtain better GPA scores by the end of their first year. As discussed by Lindo et al. (2010), the campuses are indeed different in their student composition. Campus 1 is the central campus and has a more traditional university structure, lower acceptance rates and more full-time students, while campuses 2 and 3 are satellite campuses and resemble community colleges more, with a higher acceptance rate and more part-time and commuter students. These differences suggest not only that the expected second-year GPA should differ across campuses, but also that the probation policy could have differential impacts between campuses.

In order to determine the appropriate prior parameters for this sample, we perform the prior

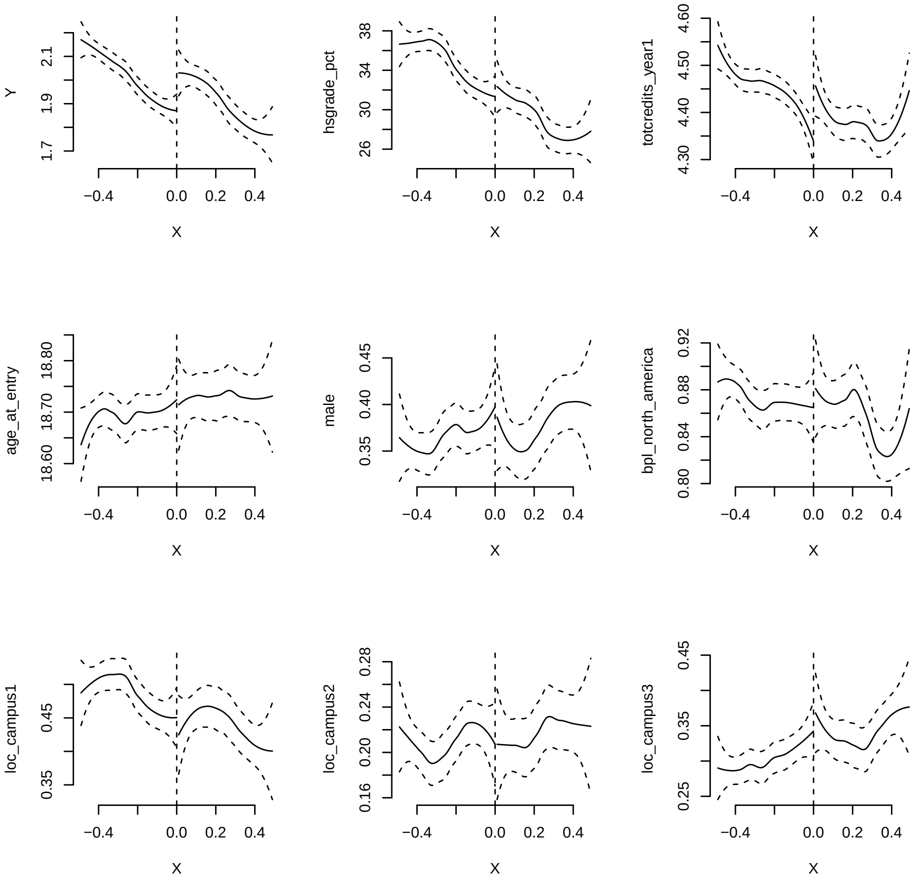

Figure 7: Outcome and covariate distribution conditional on X

Table 6: Summary statistics

	Sample	Mean	SD	Min	Max	Cor
Y	Full	2.571	0.91	0	4.3	1
	Campus 1	2.676	0.897	0	4.3	1
	Campus 2	2.486	0.886	0	4.3	1
	Campus 3	2.369	0.921	0	4.3	1
X	Full	-0.961	0.864	-2.8	1.6	-0.656
	Campus 1	-1.113	0.83	-2.8	1.5	-0.652
	Campus 2	-0.79	0.84	-2.8	1.5	-0.64
	Campus 3	-0.706	0.881	-2.7	1.6	-0.642
hsgrade_pct	Full	51.003	28.712	1	100	0.47
	Campus 1	60.282	26.021	1	100	0.456
	Campus 2	37.165	27.057	1	100	0.488
	Campus 3	37.878	27.074	1	100	0.437
totcredits_year1	Full	4.584	0.505	3	6.5	0.222
	Campus 1	4.694	0.435	4	6.5	0.191
	Campus 2	4.465	0.47	4	6	0.129
	Campus 3	4.395	0.609	3	6	0.237
age_at_entry	Full	18.656	0.735	17	21	-0.09
	Campus 1	18.631	0.72	17	21	-0.089
	Campus 2	18.658	0.717	17	21	-0.061
	Campus 3	18.716	0.781	17	21	-0.09
male	Full	0.38	0.485	0	1	-0.039
	Campus 1	0.378	0.485	0	1	-0.039
	Campus 2	0.363	0.481	0	1	-0.055
	Campus 3	0.398	0.489	0	1	-0.024
bpl_north_america	Full	0.87	0.337	0	1	0.02
	Campus 1	0.874	0.332	0	1	0.012
	Campus 2	0.897	0.305	0	1	0.02
	Campus 3	0.84	0.367	0	1	0.022

Sample size

Total: 40582; Campus 1: 23999; Campus 2: 7029; Campus 3: 9554 elicitation procedure described in section 3.4: fix X, W, generate 10 samples of the DGP described in that section, take a grid of candidate values for (N_{Omin}, N_{Opct}, h) and calculate the RMSE over the 10 synthetic samples for each combination in the grid[9]. Table 7 presents the results of this procedure. We set the parameters at the values which yield the lowest RMSE: $(N_{Omin}, N_{Opct}, h) = (5, 0.6, 0.1)$.

Table 7: Results from prior elicitation

N_{Omin}	N_{Opct}	h	RMSE
5	0.6	0.1	0.094
5	0.8	0.15	0.096
10	0.8	0.15	0.107
10	0.6	0.1	0.126
5	0.7	0.15	0.247
10	0.7	0.15	0.247
5	0.6	0.15	0.252
10	0.6	0.15	0.254
5	0.7	0.1	0.331
5	0.6	0.05	0.343
10	0.8	0.05	0.347
5	0.8	0.05	0.349
5	0.7	0.05	0.353
10	0.7	0.05	0.357
10	0.7	0.1	0.358
10	0.6	0.05	0.368
5	0.8	0.1	0.391
10	0.8	0.1	0.398

The model is fit for the whole sample but the treatment effect function at the cutoff is predicted only for the points inside the identification strip. Table 8 presents summary statistics for this prediction sample. Second-year GPA is consistently greater for treated units overall and per campus. Besides that, gender is the only feature that exhibits some difference between treatment groups, with 40.4% untreated and 26.4% treated men in campus 2, while the gender distribution for campus 1 and 3 is similar across treatment groups. The only feature that differs significantly across campuses is the high-school grade percentile: campus 1 is composed of students which had better high-school performance than those of campus 2 or 3, which are similar in that regard. Generally, the prediction sample presents a similar feature distribution across treatment groups and campuses, with the exception of high-school performance for campus 1 and gender for campus 2.

We generate 100 draws from the individual-level posterior distribution which, averaging over observations, lead to 100 draws from the ATE posterior distribution. Table 9 presents a summary of the ATE posterior. The distribution is centered at 0.14 with all the posterior mass above zero, indicating strong evidence for positive effects of the probation policy. The 95% credible interval suggests the average effect can be as low as 0.08 and as high as 0.217[10].

We now discuss heterogeneity in the BART-RDD posterior distribution. Figure 8 presents a regression tree fit to posterior point estimates of the individual effects as a summarization tool. The

[9] Because of the sample size of over 40,000 points, we are able to explore the prior reasonably with as few as 10 synthetic samples; for data with smaller sample sizes, more synthetic samples might be necessary to clearly distinguish between the candidates.

[10] For comparison, appendix section B presents the ATE results for the other estimators analyzed in the simulation exercise.

Table 8: Summary statistics - identification strip

		Control		Treatment	
Y	Sample	Mean	SD	Mean	SD
	Full	1.896	0.818	2.023	0.787
	Campus 1	1.931	0.847	2.007	0.808
	Campus 2	1.941	0.846	2.128	0.685
	Campus 3	1.823	0.756	1.976	0.819
X	Full	-0.042	0.031	0.051	0.026
	Campus 1	-0.042	0.031	0.051	0.026
	Campus 2	-0.041	0.031	0.053	0.025
	Campus 3	-0.041	0.03	0.048	0.027
hsgrade_pct	Full	31.941	22.796	31.234	22.781
	Campus 1	42.354	22.233	43.041	22.402
	Campus 2	23.399	19.246	20.95	17.759
	Campus 3	23.494	19.698	22.475	18.668
totcredits_year1	Full	4.375	0.539	4.418	0.547
	Campus 1	4.494	0.459	4.588	0.446
	Campus 2	4.367	0.456	4.434	0.457
	Campus 3	4.225	0.638	4.184	0.633
age_at_entry	Full	18.715	0.753	18.727	0.745
	Campus 1	18.708	0.731	18.701	0.712
	Campus 2	18.679	0.71	18.711	0.678
	Campus 3	18.746	0.806	18.773	0.826
male	Full	0.387	0.487	0.362	0.481
	Campus 1	0.38	0.486	0.396	0.49
	Campus 2	0.404	0.492	0.264	0.442
	Campus 3	0.387	0.488	0.38	0.486
bpl_north_america	Full	0.861	0.346	0.88	0.325
	Campus 1	0.865	0.342	0.865	0.342
	Campus 2	0.908	0.289	0.925	0.265
	Campus 3	0.828	0.378	0.872	0.335

Sample size (control/treatment):

Total: 1038/719; Campus 1: 466/318; Campus 2: 218/159; Campus 3: 354/242

Table 9: BART-RDD posterior summary for the ATE

Mean	SD	2.5%	97.5%	Median	Min	Max
0.140	0.036	0.080	0.217	0.140	0.068	0.253

summary trees are fit for the full sample and per campus. High-school performance is flagged as an important moderator for the full sample. Looking into each campus separately reveals more heterogeneity. For students who performed poorly in high-school in campus 1, we see additional moderation by birth place and credits attempted in the first year. In campus 2, we can see that the effect for women is larger than for men among those who feature above the 31-st percentile of high-school grades. Finally, for campus 3, the most important moderators are gender, birth place and age at entry.

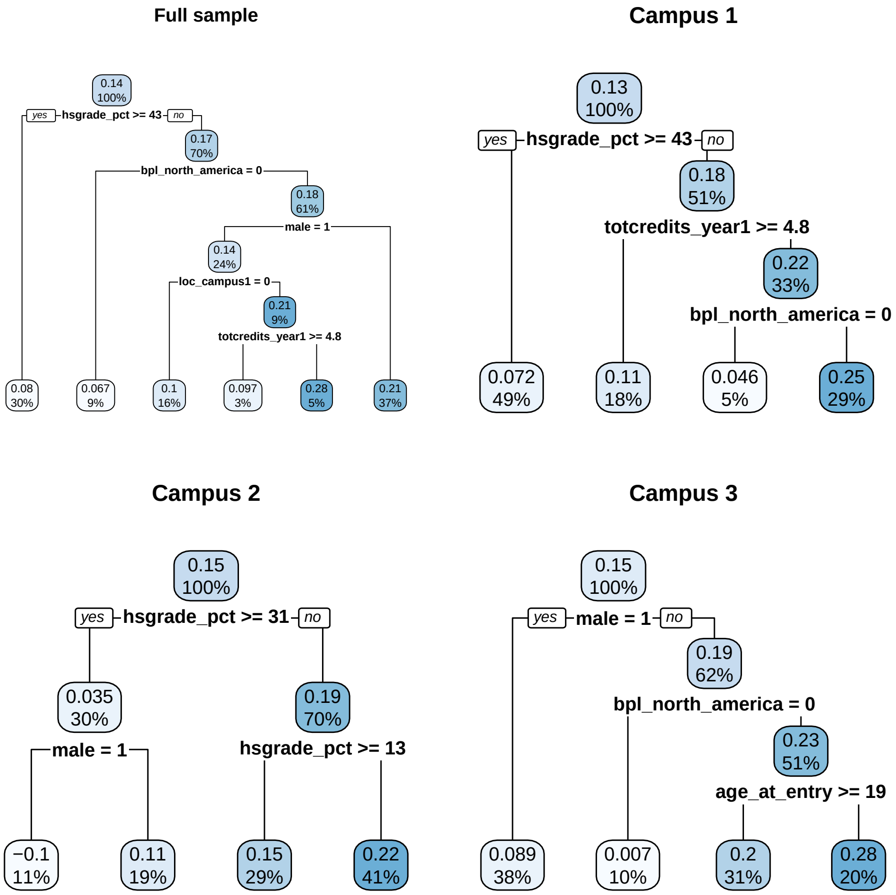

Figure 8: Regression tree fit to posterior point estimates of individual treatment effects: top number in each box is the average subgroup treatment effect, lower number shows the percentage of the total sample in that subgroup; the full sample summary flags high-school performance, birth place, gender, campus location and credits in first year as important moderators; the separate campus fits indicate heterogeneity between the campuses: for campus 1, high-school performance, credits attempted and birth place are flagged as important moderators, while for campus 2, high-school performance and gender are important and, for campus 3, gender, birth place and age at entry are the important moderators

The results described so far are consistent with those presented by Lindo et al. (2010), both in magnitude and, to some degree, in potential sources of treatment effect heterogeneity. In particular, the authors also find a greater effect for students who performed below average in high-school and for women. Our posterior predictions however flag additional features as potential moderators, such as age at entry, birth place and campus, which highlights how depending on pre-specification of relevant subgroups might lead researchers to miss other interesting features of the data. Lindo et al. (2010) note that interpreting these results as true effects requires caution since there is evidence that the probation policy leads to differential dropout rates, which changes the composition of students before and after the evaluation of first-year GPA. However, further discussion on this topic is out of the scope of this project.

We conclude this section with an illustration of how to perform posterior inference about heterogeneity in the effects with the results of our model. Based on the moderators flagged by the summarization trees, we investigate the posterior difference in treatment effects across some subgroups. The first panel in figure 9 presents the posterior difference between students in the bottom 43% versus those in the upper 57% of the high-school grade distribution for campus 1. There is a 92% posterior probability that the treatment effect is larger for the former group. The second panel presents a similar analysis for campus 2, where the threshold was the 31-st percentile of the high-school grade distribution. There is also strong evidence for a larger effect for students lower in that distribution, with a posterior probability of a larger effect of 95%. The third panel presents the posterior difference for students who entered college younger than 19 versus those who entered older than that in campus 3. There is also strong evidence of a larger effect for the former group, with posterior probability of 84%. Finally, the last panel presents the posterior difference in average effects between each campus. The biggest difference is between campus 3 and campus 1, in which case there is a 66% probability of a larger effect for the former. There is a 59% posterior probability that the effect is larger for campus 2 than campus 1 and a 54% posterior probability that the effect is larger for campus 3 than campus 2.

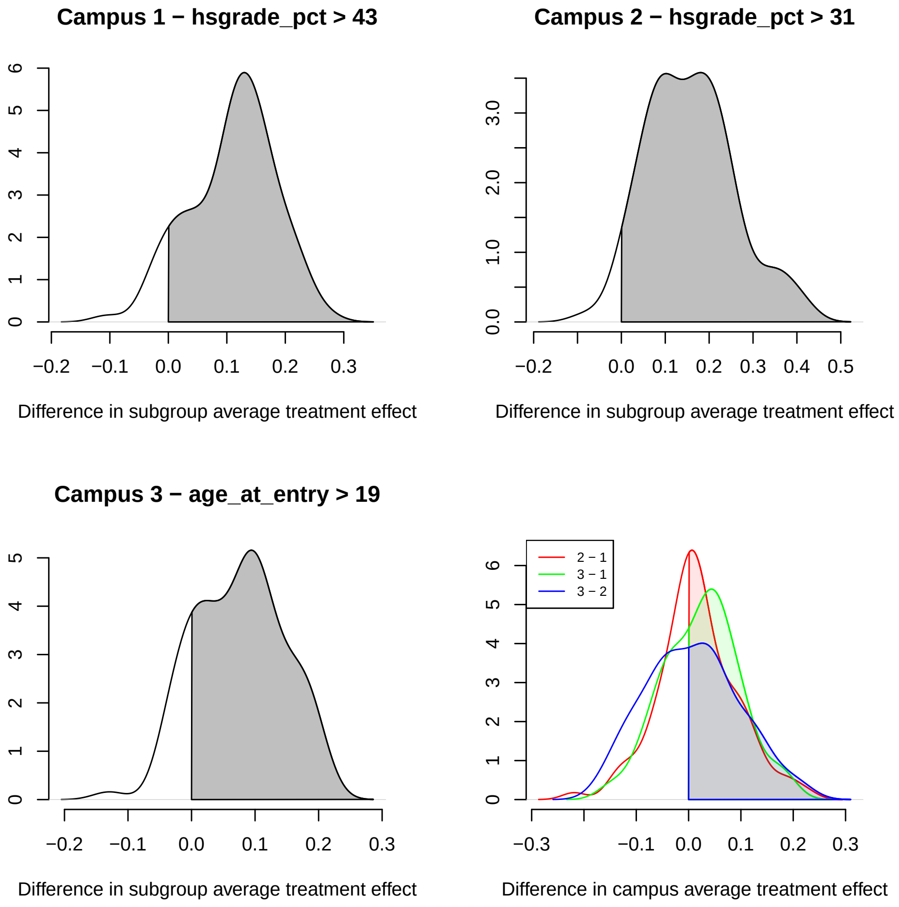

Figure 9: Differences in subgroup treatment effects: the first panel shows the posterior difference between students below and above the 43-rd percentile of high-school grades respectively in campus 1, which has a 92% posterior mass above 0; the second panel performs the same analysis for the 31-st percentile of high-school grades for students in campus 2, which has a 95% posterior mass above 0; the third panel presents the posterior difference between students that got into college younger versus older than 19 in campus 3, which has a posterior mass of 84% above 0; the last panel presents the posterior differences in the ATE between each campus: there is a 66% posterior probability of a larger effect for campus 3 compared to campus 1, a 59% probability for a larger effect on campus 2 compared to campus 1 and a 54% probability of a larger effect on campus 3 compared to campus 2

References

Arai, Y., Otsu, T., and Seo, M. H. (2021). Regression discontinuity design with potentially many covariates. *arXiv preprint arXiv:2109.08351*.

Becker, S. O., Egger, P. H., and Von Ehrlich, M. (2013). Absorptive capacity and the growth and investment effects of regional transfers: A regression discontinuity design with heterogeneous treatment effects. *American Economic Journal: Economic Policy*, 5(4):29–77.

Bertanha, M. (2020). Regression discontinuity design with many thresholds. *Journal of Econometrics*, 218(1):216–241.

Branson, Z., Rischard, M., Bornn, L., and Miratrix, L. W. (2019). A nonparametric bayesian methodology for regression discontinuity designs. *Journal of Statistical Planning and Inference*, 202:14–30.

Calonico, S., Cattaneo, M. D., Farrell, M. H., and Titiunik, R. (2019). Regression discontinuity designs using covariates. *Review of Economics and Statistics*, 101(3):442–451.

Calonico, S., Cattaneo, M. D., and Titiunik, R. (2015). rdrobust: An r package for robust nonparametric inference in regression-discontinuity designs. *R J.*, 7(1):38.

Cattaneo, M. D., Titiunik, R., Vazquez-Bare, G., and Keele, L. (2016). Interpreting regression discontinuity designs with multiple cutoffs. *The Journal of Politics*, 78(4):1229–1248.

Chib, S., Greenberg, E., and Simoni, A. (2023). Nonparametric bayes analysis of the sharp and fuzzy regression discontinuity designs. *Econometric Theory*, 39(3):481–533.

Chipman, H. A., George, E. I., and McCulloch, R. E. (1998). Bayesian cart model search. *Journal of the American Statistical Association*, 93(443):935–948.

Chipman, H. A., George, E. I., McCulloch, R. E., et al. (2010). Bart: Bayesian additive regression trees. *The Annals of Applied Statistics*, 4(1):266–298.

Frandsen, B. R., Frölich, M., and Melly, B. (2012). Quantile treatment effects in the regression discontinuity design. *Journal of Econometrics*, 168(2):382–395.

Frölich, M. and Huber, M. (2019). Including covariates in the regression discontinuity design. *Journal of Business & Economic Statistics*, 37(4):736–748.

Hahn, J., Todd, P., and Van der Klaauw, W. (2001). Identification and estimation of treatment effects with a regression-discontinuity design. *Econometrica*, 69(1):201–209.

Hahn, P. R., Murray, J. S., Carvalho, C. M., et al. (2020). Bayesian regression tree models for causal inference: regularization, confounding, and heterogeneous effects. *Bayesian Analysis*.

He, J. and Hahn, P. R. (2023). Stochastic tree ensembles for regularized nonlinear regression. *Journal of the American Statistical Association*, 118(541):551–570.

Hill, J. L. (2011). Bayesian nonparametric modeling for causal inference. *Journal of Computational and Graphical Statistics*, 20(1):217–240.

Hsu, Y.-C. and Shen, S. (2019). Testing treatment effect heterogeneity in regression discontinuity designs. *Journal of Econometrics*, 208(2):468–486.

Imbens, G. and Kalyanaraman, K. (2012). Optimal bandwidth choice for the regression discontinuity estimator. *The Review of economic studies*, 79(3):933–959.

Imbens, G. W. and Lemieux, T. (2008). Regression discontinuity designs: A guide to practice. *Journal of econometrics*, 142(2):615–635.

Karabatsos, G. and Walker, S. G. (2015). A bayesian nonparametric causal model for regression discontinuity designs. In *Nonparametric Bayesian Inference in Biostatistics*, pages 403–421. Springer.

Krantsevich, N., He, J., and Hahn, P. R. (2023). Stochastic tree ensembles for estimating heterogeneous effects. In *International Conference on Artificial Intelligence and Statistics*, pages 6120–6131. PMLR.

Kreiss, A. and Rothe, C. (2023). Inference in regression discontinuity designs with high-dimensional covariates. *The Econometrics Journal*, 26(2):105–123.

Künzel, S. R., Sekhon, J. S., Bickel, P. J., and Yu, B. (2019). Metalearners for estimating heterogeneous treatment effects using machine learning. *Proceedings of the national academy of sciences*, 116(10):4156–4165.

Lee, D. S. and Lemieux, T. (2010). Regression discontinuity designs in economics. *Journal of economic literature*, 48(2):281–355.

Lindo, J. M., Sanders, N. J., and Oreopoulos, P. (2010). Ability, gender, and performance standards: Evidence from academic probation. *American Economic Journal: Applied Economics*, 2(2):95–117.

Reguly, A. (2021). Heterogeneous treatment effects in regression discontinuity designs. *arXiv preprint arXiv:2106.11640*.

Shen, S. and Zhang, X. (2016). Distributional tests for regression discontinuity: Theory and empirical examples. *Review of Economics and Statistics*, 98(4):685–700.

Thistlethwaite, D. L. and Campbell, D. T. (1960). Regression-discontinuity analysis: An alternative to the ex post facto experiment. *Journal of Educational psychology*, 51(6):309.

A Prior calibration experiments

Algorithm 2 describes the procedure in pseudocode form. It is worth emphasizing that the particular functional form choices and parameter values for the synthetic data can be changed to better fit certain applications, although we recommend following the same general structure.

```
Algorithm 2: Prior elicitation procedure
  Input: Set of candidate prior parameter values $\Theta$, where $\theta \in \Theta$ is a 3-tuple $(h, \alpha, N_{Omin})$
  Output: Chooses $\theta^* \in \Theta$ to fit BART-RDD for the full sample $(Y, X, W)$
  Data: Running variable and additional features, $(X, W)$
  Generate $S$ samples of a synthetic outcome as follows:
      $\mu(X, W) = \frac{1}{P} \sum_{p=1}^{P} W_p + \frac{1}{1 + \exp(-5X)}$
      $\tau(X) = \bar{\tau} - \frac{\log(1 + X)}{50}$
      $\bar{\tau} = 0.4$
      $Y_s = \mu(X, W) + \tau(X) Z + \varepsilon_s$
      $\varepsilon_s \sim \mathrm{N}(0, 1)$
  for $\theta \in \Theta$ do
      for $s \in S$ do
          Fit BART-RDD for sample $(Y_s, X, W)$ with prior parameters $\theta$
      end
      Calculate $RMSE_\theta$ as the root-mean-square error of the ATE point estimates produced
        by BART-RDD for each of the S samples
  end
  Choose $\theta^*$ which leads to the lowest $RMSE_\theta$
```

To illustrate this procedure, suppose we observe one sample of (X, W) of size 1000 from the DGP analyzed in the simulations[11]. For that sample, we generate $S = 20$ samples of Y_s from a synthetic DGP constructed as described in algorithm 2. For the set of parameter candidates we consider $h \in \{0.05, 0.1, 0.15, 0.2\}$, $N_{Omin} \in \{1, 5, 10\}$ and $\alpha \in \{0.6, 0.75, 0.9\}$. Figure 10 presents the results of our exploration.

Although the RMSE patterns observed are specific to this sample, close inspection of figure 10 allows us to observe some trends that can reasonably be expected to hold in many cases. Consider first the setup with small h. In this scenario, the nodes that include the identification strip are likely to be small unless the sample is well populated with points very close to the cutoff. One consequence is that, if we allow for nodes with only one point from each side of the cutoff in the strip (*i.e.* $N_{Omin} = 1$), we might end up with nodes that are very small, in which case our estimates are very unlikely to move away from the prior, which will generally lead to poor ATE estimates unless this parameter is also very small. Increasing N_{Omin} safeguards against this possibility, as this would ensure the nodes are not that small. This is made clear by the fact that greater values for N_{Omin} are uniformly better up until $h = 0.1$.

Focusing next on the larger values of h, we see that $h = 0.2$ is the setup that leads to the most sensitivity of the prior to the other parameters. Graphically, we see that the lines for each value of N_{Omin} are less ‘clumped’ together than for the lower values of h, meaning the combinations of

[11] Note that, although there are several variations of the DGP considered in the simulations, the distribution of (X, W) are always the same

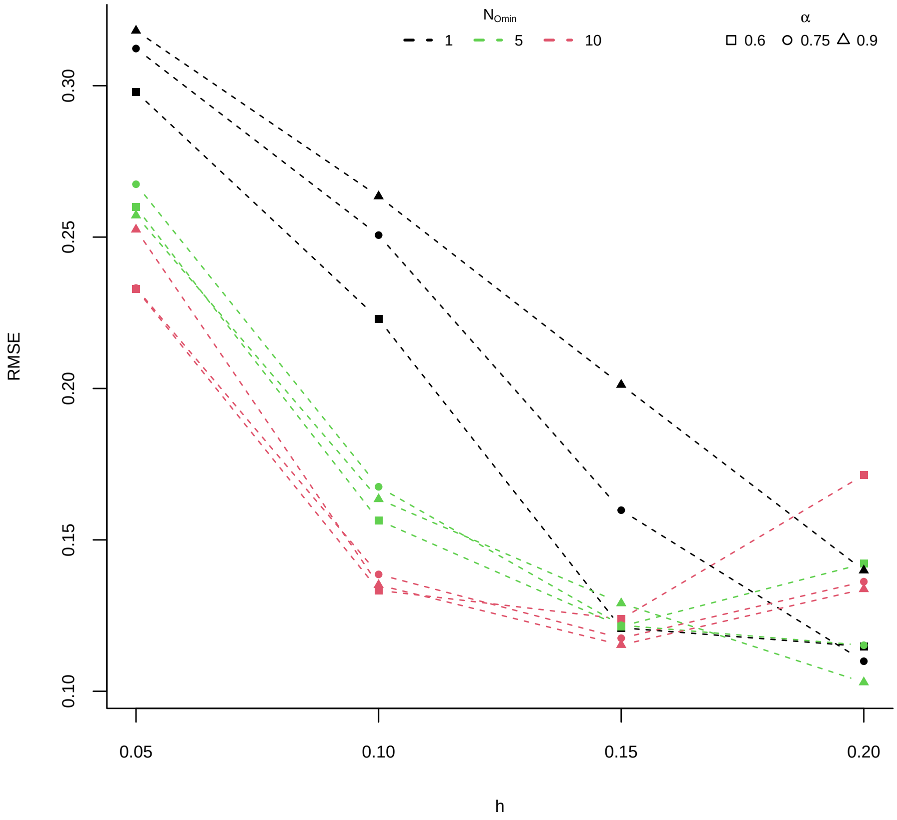

Figure 10: RMSE for each candidate (h, α, N_{Omin})

(α, N_{Omin}) lead to more varied results now. Practically, greater h values mean we are using points that are potentially too far away from the cutoff for the ATE predictions at that point, which could evidently bias the results. In that case, lower α means we allow even more points far from the cutoff to influence these predictions, since we obtain nodes that may contain many points far from the identification strip. This can be seen in the figure since, for $h = 0.2$, greater values of α generally produce the best results.

Overall, figure 10 suggests setting h and N_{Omin} appropriately is crucial, while α can be set to offset any bias that might occur for a given combination of the other parameters. For this example, setting $N_{Omin} = 10$ and $h = \{0.1, 0.15\}$ seems reasonable. Then, we can set α accordingly. For example, if we choose $h = 0.1$, setting $\alpha = 0.6$ is best, although the other values lead to very similar results. In comparison, if we set $h = 0.15$, greater α is uniformly better, as this value of h seems to be large enough for this sample that we should trim the outter regions of the identification strip more strictly. However, the results are again not sensitive to α when $h = 0.15$. Finally, it is worth noting that, although the lowest RMSE is achieved with $(h, \alpha, N_{Omin}) = (0.2, 5, 0.9)$, we advise against setting $h = 0.2$ for this sample given the much greater sensitivity of the prior to the other parameters in this case. Since one can never really know how close this synthetic DGP is to the real one, the search for the lowest RMSE here should be moderated by considering the sensitivity of the prior as well. With these considerations in mind, we suggest setting $(h, \alpha, N_{Omin}) = (0.1, 10, 0.6)$ for this sample, which is the setup we use for the simulations.

B Application results for other estimators

This section presents the ATE estimates for the Lindo et al. (2010) data produced by the estimators studied in our simulations. S-BART and T-BART present evidence of a near zero effect and the polynomial estimators suggest a similar effect magnitude to BART-RDD. It is worth noting that BART-based models have a regularization component, which could explain why the predictions from this models are more conservative than those of the polynomial estimators (although only slightly so for BART-RDD).

Table 10: ATE point estimate and 95% confidence interval for different estimators

S-BART	T-BART	LLR	CGS
0.074	0.062	0.205	0.176
(-0.013,0.129)	(0,0.117)	(0.127,0.282)	(0.019,0.323)